

**EFFECTS OF TEMPERATURE DEPENDENT THERMAL
CONDUCTIVITY ON THE COUPLING OF CONDUCTION AND
JOULE HEATING WITH MAGNETOHYDRODYNAMIC FREE
CONVECTION FLOW ALONG A VERTICAL FLAT PLATE**



REHENA NASRIN
Student No. 100609015P
Registration No.100609015, Session: October-2006

**MASTER OF PHILOSOPHY
IN
MATHEMATICS**



Department of Mathematics
Bangladesh University of Engineering & Technology
Dhaka-1000, Bangladesh
August - 2009

The thesis titled

**EFFECTS OF TEMPERATURE DEPENDENT THERMAL CONDUCTIVITY
ON THE COUPLING OF CONDUCTION AND JOULE HEATING WITH
MAGNETOHYDRODYNAMIC FREE CONVECTION FLOW ALONG A
VERTICAL FLAT PLATE**

Submitted by

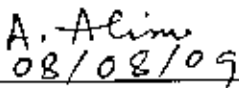
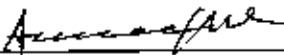
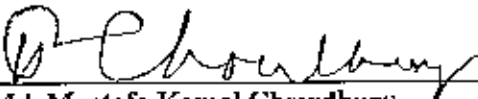
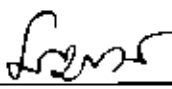
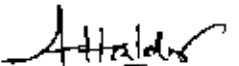
REHENA NASRIN

Student No.100609015P, Registration No.100609015, Session: October-2006, a part-time student of M. Phil. (Mathematics) has been accepted as satisfactory in partial fulfillment for the degree of

Master of Philosophy in Mathematics

on August 08, 2009

BOARD OF EXAMINERS

1. 
_____ Chairman
(Supervisor)
Dr. Md. Abdul Alim
Associate Professor
Department of Mathematics, BUET, Dhaka
2. 
_____ Member
(Ex-Officio)
Head
Department of Mathematics, BUET, Dhaka
3. 
_____ Member
Dr. Md. Mustafa Kamal Chowdhury
Professor
Department of Mathematics, BUET, Dhaka
4. 
_____ Member
Dr. Md. Manirul Alam Sarker
Professor
Department of Mathematics, BUET, Dhaka
5. 
_____ Member
(External)
Dr. Amal Krishna Halder
Professor
Department of Mathematics
University of Dhaka.

DEDICATION

**This work is dedicated
To
My dearest daughters**

Abstract

In this dissertation, the effects of temperature dependent thermal conductivity on the coupling of conduction and Joule heating with viscous dissipation and Magneto hydrodynamic free convection flow along a vertical flat plate have been investigated numerically. A steady laminar two dimensional MHD free convection flow is considered here. The governing equations contain the equation of continuity, momentum and energy. These equations with associated boundary conditions for this phenomenon are converted to dimensionless form using suitable transformations. The transformed non-linear ordinary differential equations are then solved using the implicit finite difference method with Keller-box scheme. FORTRAN 90 is used to perform computational job and the post processing software TECPLOT has been used to display the numerical results graphically.

The results in terms of skin friction and surface temperature profile for Joule heating parameter J and viscous dissipation parameter N are shown in tabular form. Numerical results of the velocity profile, temperature profile, skin friction coefficient and surface temperature profiles have been exhibited graphically for different values of the magnetic parameter M , thermal conductivity variation parameter γ , viscous dissipation parameter N , Joule heating parameter J separately and the Prandtl number Pr as well.

Author's Declaration

I, hereby declare that this thesis work has submitted to the Department of Mathematics, Bangladesh University of Engineering and Technology (BUET) in partial fulfillment of the requirements for the degree of Master of Philosophy in Mathematics. The work is also original except where indicated by and attached with special reference in the context. This dissertation has not been submitted elsewhere (Universities or Institutions) for the any other degree either in home or abroad



(Rehana Nasrin)

Date: 8th August, 2009

Acknowledgements

At first all Praise belongs to The "Almighty ALLAH", the most merciful, munificent to men and His exploit.

I would like to express heartiest gratitude to my supervisor Dr. Md. Abdul Alim, Associate Professor, Department of Mathematics, BUET, Dhaka for his good guidance, support, valuable suggestions, constant inspiration and supervision during the research work of the M. Phil. Program.

I express my deep regards to Prof. Dr. Md. Abdul Maleque, head, Department of Mathematics, Prof. Dr. Md. Mustafa Kamal Chowdhury, the former head of the Department of Mathematics, Prof. Dr. Md. Manirul Alam Sarker and Prof. Dr. Md. Abdul Hakim Khan, Department of Mathematics, BUET, Dhaka for their wise and liberal co-operation in providing me all necessary help from the department during my course of M. Phil. Program. I would also like to extend my thanks to all my respectable teachers, Department of Mathematics, BUET, Dhaka for their constant encouragement.

I am very grateful to my beloved husband who guided and helped me morally and spiritually. Special thanks to my colleagues who had tremendously and positively inspired me.

I must acknowledge my debt to my parents for whom I have been able to see the beautiful sights and sounds of the world.

Contents

Abstract	iv
Author's Declaration	v
Acknowledgements	vi
Nomenclature	viii
List of Figures	x
List of Tables	xii
Chapter 1	1
1.1 Introduction	1
1.2 Literature Survey	4
Chapter 2	7
Effects of Variable Thermal Conductivity on the Coupling of Conduction and Joule Heating with Magnetohydrodynamic Free Convection Flow along a Vertical Flat Plate	7
2.1 Introduction	7
2.2 Governing equations of the flow	7
2.3 Transformation of the governing equations	10
2.4 Results and Discussion	12
2.5 Conclusion	24
Chapter 3	25
Combined Effects of Variable Thermal Conductivity and Joule Heating on MHD Free Convection Flow along a Vertical Flat Plate with Conduction and Viscous Dissipation	25
3.1 Introduction	25
3.2 Governing equations of the flow	25
3.3 Transformation of the governing equations	26
3.4 Results and Discussion	29
3.5 Comparison of effect of N	37
3.6 Conclusion	43
Chapter 4	44
4.1 Conclusion	44
4.2 Extension of this work	45
References	46
Appendix	49
Implicit Finite Difference Method	49

Nomenclature

b	Plate thickness
\vec{B}	Magnetic induction vector
C_{fs}	Local skin friction coefficient
C_p	Specific heat at constant pressure
\vec{F}	Body force per unit volume
f	Dimensionless stream function
g	Acceleration due to gravity
Gr	Grashof number
h	Dimensionless temperature
H_0	Applied Magnetic field strength
\vec{J}	Current density vector
J	Joule heating parameter
l	Length of the plate
L	Reference length
M	Magnetic parameter
N	Viscous dissipation parameter
P	Conjugate conduction parameter
Pr	Prandtl number
T	Temperature of the interface
T_b	Temperature at outside surface of the plate
T_f	Temperature of the fluid
T_∞	Temperature of the ambient fluid
\vec{u}	Velocity component along \vec{x} - direction
\vec{v}	Velocity component along \vec{y} - direction
$\vec{V} \times \vec{B}$	Electrical fluid vector
u	Dimensionless velocity component along x - direction
v	Dimensionless velocity component along y - direction
\vec{x}	Cartesian co-ordinates
\vec{y}	Cartesian co-ordinates
x	Dimensionless Cartesian co-ordinates
y	Dimensionless Cartesian co-ordinates

Greek Symbols

β	Co-efficient of thermal expansion
γ	Thermal conductivity variation parameter
∇	Vector differential operator
δ	Constant
η	Similarity variable
$\theta(x, 0)$	Surface temperature profile
κ_{∞}	Thermal conductivity of the ambient fluid
κ_s	Thermal conductivity of the solid
κ_f	Thermal conductivity of the fluid
μ	Viscosity of the fluid
μ_e	Magnetic permeability of the fluid
ν	Kinematic viscosity
ρ	Density of the fluid inside the boundary layer
σ	Electrical conductivity of the fluid
τ_w	Shearing stress
ψ	Stream function

List of Figures

Figure 2.2	Variation of velocity profile against η for varying of M with $\gamma = 0.10, J = 0.07$ and $Pr = 0.73$	13
Figure 2.3	Variation of temperature profile against η for varying of M with $\gamma = 0.10, J = 0.07$ and $Pr = 0.73$	13
Figure 2.4	Variation of velocity profile against η for varying of γ with $M = 0.10, J = 0.01$ and $Pr = 0.73$	14
Figure 2.5	Variation of temperature profile against η for varying of γ with $M = 0.01, J = 0.01$ and $Pr = 0.73$	14
Figure 2.6	Variation of velocity profile against η for varying of Pr with $M = 0.10, J = 0.07$ and $\gamma = 0.10$	16
Figure 2.7	Variation of temperature profile against η for varying of Pr with $M = 0.10, J = 0.07$ and $\gamma = 0.10$	16
Figure 2.8	Variation of velocity profile against η for varying of J with $M = 0.01, Pr = 0.73$ and $\gamma = 0.01$	17
Figure 2.9	Variation of temperature profile against η for varying of J with $M = 0.01, Pr = 0.73$ and $\gamma = 0.01$	17
Figure 2.10	Variation of skin friction coefficient against x for varying of M with $\gamma = 0.10, J = 0.07$ and $Pr = 0.73$	19
Figure 2.11	Variation of surface temperature profile against x for varying of M with $\gamma = 0.10, J = 0.07$ and $Pr = 0.73$	19
Figure 2.12	Variation of skin friction coefficient against x for varying of γ with $M = 0.10, J = 0.01$ and $Pr = 0.73$	20
Figure 2.13	Variation of surface temperature profile against x for varying of γ with $M = 0.01, J = 0.01$ and $Pr = 0.73$	20
Figure 2.14	Variation of skin friction coefficient against x for varying of Pr with $M = 0.10, J = 0.07$ and $\gamma = 0.10$	21
Figure 2.15	Variation of surface temperature profile against x for varying of Pr with $M = 0.10, J = 0.07$ and $\gamma = 0.10$	21
Figure 2.16	Variation of skin friction coefficient against x for varying of J with $M = 0.01, Pr = 0.73$ and $\gamma = 0.01$	22
Figure 2.17	Variation of surface temperature profile against x for varying of J with $M = 0.01, Pr = 0.73$ and $\gamma = 0.01$	22
Figure 3.2	Variation of velocity profile against η for varying of Pr with $M = 0.02, N = 0.02, J = 0.01$ and $\gamma = 0.1$	30
Figure 3.3	Variation of temperature profile against η for varying of Pr with $M = 0.02, N = 0.02, J = 0.01$ and $\gamma = 0.1$	30
Figure 3.4	Variation of velocity profile against η for varying of N with $\gamma =$	31

	0.02, $M = 2.6$, $J = 0.01$ and $Pr = 0.73$	
Figure 3.5	Variation of temperature profile against η for varying of N with $\gamma = 0.02$, $M = 2.6$, $J = 0.01$ and $Pr = 0.73$	31
Figure 3.6	Variation of velocity profile against η for varying of J with $\gamma = 0.01$, $M = 2.6$, $N = 0.01$ and $Pr = 1.73$	32
Figure 3.7	Variation of temperature profile against η for varying of J with $\gamma = 0.01$, $M = 2.6$, $N = 0.01$ and $Pr = 1.73$	32
Figure 3.8	Variation of skin friction coefficient against x for varying of Pr with $M = 0.02$, $N = 0.02$, $J = 0.01$ and $\gamma = 0.1$	34
Figure 3.9	Variation of surface temperature profile against x for varying of Pr with $M = 0.02$, $N = 0.02$, $J = 0.01$ and $\gamma = 0.1$	34
Figure 3.10	Variation of skin friction coefficient against x for varying of N with $M = 2.6$, $\gamma = 0.02$, $J = 0.01$ and $Pr = 0.73$	35
Figure 3.11	Variation of surface temperature profile against x for varying of N with $M = 2.6$, $\gamma = 0.02$, $J = 0.01$ and $Pr = 0.73$	35
Figure 3.12	Variation of skin friction coefficient against x for varying of J with $M = 2.6$, $\gamma = 0.02$, $N = 0.01$ and $Pr = 1.73$	36
Figure 3.13	Variation of surface temperature profile against x for varying of J with $M = 2.6$, $\gamma = 0.02$, $N = 0.01$ and $Pr = 1.73$	36
Figure 3.14	Variation of velocity profile against x for varying of γ with $M = 0.01$, $J = 0.01$, $Pr = 0.73$ and $N = 0.0$	38
Figure 3.15	Variation of velocity profile against x for varying of γ with $M = 0.01$, $J = 0.01$, $Pr = 0.73$ and $N = 0.1$	38
Figure 3.16	Variation of temperature profile against η for varying of γ with $M = 0.01$, $J = 0.01$, $Pr = 0.73$ and $N = 0.0$	39
Figure 3.17	Variation of temperature profile against η for varying of γ with $M = 0.01$, $J = 0.01$, $Pr = 0.73$ and $N = 0.1$	39
Figure 3.18	Variation of skin friction coefficient against η for varying of γ with $M = 0.01$, $J = 0.01$, $Pr = 0.73$ and $N = 0.0$	40
Figure 3.19	Variation of skin friction coefficient against η for varying of γ with $M = 0.01$, $J = 0.01$, $Pr = 0.73$ and $N = 0.1$	40
Figure 3.20	Variation of surface temperature profile against η for varying of γ with $M = 0.01$, $J = 0.01$, $Pr = 0.73$ and $N = 0.0$	41
Figure 3.21	Variation of surface temperature profile against η for varying of γ with $M = 0.01$, $J = 0.01$, $Pr = 0.73$ and $N = 0.1$	41
Figure A-1	Net rectangle of difference approximations for the Box scheme.	50

List of Tables

Table 2.1	Comparison of the present numerical results of surface temperature profile with Prandtl number $Pr = 0.733$, $M = 0.0$, $J = 0.0$ and $\gamma = 0.0$	23
Table 2.2	Comparison of the present numerical results of skin friction coefficient with Prandtl number $Pr = 0.733$, $M = 0.0$, $J = 0.0$ and $\gamma = 0.0$	23
Table 2.3	Skin friction coefficient and surface temperature profile against x for different values of Joule heating parameter J with other controlling parameters $\gamma = 0.01$, $M = 0.01$ and $Pr = 0.73$	24
Table 3.1	Skin friction coefficient and surface temperature profile against x for different values of viscous dissipation parameter N with other controlling parameters $M = 2.6$, $\gamma = 0.02$, $J = 0.01$ and $Pr = 0.73$	33
Table 3.2	Comparison of skin friction coefficient against x for different values of thermal conductivity variation parameter γ (with and without effect of N) having other controlling parameters $M = 0.01$, $J = 0.01$ and $Pr = 0.73$	42



Chapter 1

1.1 Introduction

The natural convection procedures are governed essentially by three features namely the body force, the temperature difference in the flow field and the fluid density variations with temperature. Natural convection is the most important mode of heat transfer from pipes, transmission lines, refrigerating coils, burning radiators and various other situations. The manipulation of natural convection heat transfer can be deserted in the case of large Reynolds number and very small Grashof number. Alternatively, the natural convection should be the governing aspect for large Grashof number and small Reynolds number.

Flow of electrically conducting fluid in presence of magnetic field and the effect of temperature dependent thermal conductivity on the coupling of conduction and Joule heating with natural convection problems are important from the technical point of view. Such types of problems have received much attention by many researchers. Experimental and theoretical works on MHD free and forced convection flows have been done extensively but a few works have been done on the conjugate effects of convection and conduction problems.

It is possible to attain equilibrium in a conducting fluid if the current is parallel to the magnetic field. Then the magnetic forces vanish and the equilibrium of the gas is the same as in the absence of magnetic fields. But most liquids and gases are poor conductors of electricity. In the case when the conductor is either a liquid or a gas, electromagnetic forces will be generated which may be of the same order of magnitude as the hydrodynamical and inertial forces. Thus the equation of motion as well as the other forces will have to take these electromagnetic forces into account. The MHD was originally applied to astrophysical and geophysical problems, where it is still very important but more recently applied to the problem of fusion power where the application is the creation and containment of hot plasmas by electromagnetic forces, since material walls would be destroyed.

Magnetohydrodynamics is that branch of science, which deals with the motion of highly conducting ionized (electric conductor) fluid in presence of magnetic field. The motion of the conducting fluid across the magnetic field generates electric currents which change the

Introduction.

magnetic field and the action of the magnetic field on these currents give rise to mechanical forces, which modify the fluid.

The specific problem selected for the present study is the flow and heat transfer in an electrically conducting fluid adjacent to the surface. The interaction of the magnetic field and the moving electric charge carried by the flowing fluid induces a force, which tends to oppose the fluid motion and near the leading edge. The velocity is very small, so that the magnetic force which is proportional to the magnitude of the longitudinal velocity and acts in the opposite direction is also very small. Consequently, the influence of the magnetic field on the boundary layer is exerted only through induced forces within the boundary layer itself without additional effects arising from the free stream pressure gradient. Solid matter is generally excluded from MHD effects, but it should be realized that the same principles would apply.

The motion of an electrically conducting fluid, like mercury, under a magnetic field, in general, gives rise to induced electric currents on which mechanical forces are exerted by the magnetic field. On the other hand, the induced electric currents also produce induced magnetic field. Thus there is a two-way interaction between the flow field and the magnetic field, the magnetic field exerts force on the fluid by producing induced currents and the induced currents change the original magnetic field. Therefore, the magnetohydrodynamic flows (the flows of electrically conducting fluids in the presence of magnetic field) are more complex than the ordinary hydrodynamic flows

The study of temperature and heat transfer is of great importance because of its almost universal occurrence in many branches of science and engineering. Although heat transfer analysis is most important for the proper sizing of fuel elements in the nuclear reactors cores to prevent burnout. Heat transfer is commonly associated with fluid dynamics. The knowledge of temperature distribution is essential in heat transfer studies because of the fact that the heat flow takes place only whenever there is a temperature gradient in a system.

In electronics in particular and in physics broadly, Joule heating is the heating effect of conductors carrying currents. It refers to the increase in temperature of a conductor as a result of resistance to an electrical current flowing through it. At an atomic level, Joule heating is the result of moving electrons colliding with atoms in a conductor, whereupon momentum is transferred to the atom, increasing its kinetic or vibrational energy. When

Introduction.

similar collisions cause a permanent structural change, rather than an elastic response, the result is known as electro migration. Joule heating is caused by interactions between the moving particles that form the current (usually, but not always, electrons) and the atomic ions that make up the body of the conductor. Charged particles in an electric circuit are accelerated by an electric field but give up some of their kinetic energy each time they collide with an ion. The increase in the kinetic energy of the ions manifests itself as heat and a rise in the temperature of the conductor. Hence energy is transferred from electrical power supply to the conductor and any materials with which it is in thermal contact.

James Prescott Joule studied first Joule heating in 1841. It is the process by which the passage of an electric current through a conductor releases heat. Joule's first law is also known as Joule effect. It states that heat generation by a constant current through a resistive conductor for a time whose unit is joule. It is also related to Ohm's first law. Joule heating is also referred to as Ohmic heating or Resistive heating because of its relationship to Ohm's law. The SI unit of energy was subsequently named the joule and given the symbol J. The commonly known unit of power, the watt, is equivalent to one joule per second.

The heat flux, which is defined as the amount of heat transfer per unit area in per unit time, can be calculated from the physical laws relatives to the temperature gradient and the heat flux. The three different manners of heat transfer namely; conduction, convection and radiation must be considered. In reality, the combined effects of these three modes of heat transfer control temperature distribution in a medium.

Convection is the transfer of heat by the actual movement of the warmed matter. Heat leaves the coffee cup as the currents of steam and air rise. Convection is the transfer of heat energy in a gas or liquid by movement of currents. The heat moves with the fluid. Considerable convection is responsible for making macaroni rise and fall in a pot of heated water. The warmer portions of the water are less dense and therefore, they rise. Mean while, the cooler portions of the water fall because they are denser.

Conduction is the transfer of energy through matter from particle to particle. It is the transfer and distribution of heat energy from atom to atom within a substance. For example, a spoon in a cup of hot soup becomes warmer because the heat from the soup is conducted along the spoon. Conduction is most effective in solids but it can happen in fluids.

Introduction.

Thermal conductivity is the intensive property of material that indicates its ability to conduct heat. Thermal conductivity approximately tracks electrical conductivity, as freely moving electrons transfer not only electric current but also heat energy. However, the general correlation between electrical and thermal conductance does not hold for other materials due to the increased importance of photon carries for heat non-metals

Thermal conduction is the spontaneous transfer of thermal energy through matter, from a region of high temperature to a region of lower temperature. The same forces that act to support the structure of matter can be said to move by physical contact between the particles transfer and the thermal energy, in the form of continuous random motion of particles of the matter.

1.2 Literature Survey

The case of a heated isothermal horizontal surface with transpiration was discussed in some detail by Clarke and Riley (1975, 1976). The combined free and forced convection flow about inclined surfaces in porous media was studied by Chen (1977). The combined forced and free convection in boundary layer flow of a micro-polar fluid over a horizontal plate was investigated by Hassanien (1977). Similarity solutions were acquired in his work for the case of wall temperature, which is inversely proportional to the square root of the distance from the leading edge.

Takhar and Soundalgekar (1980) studied the dissipation effects on MHD free convection flow past a semi-infinite vertical plate. The effect of axial heat conduction in a vertical flat plate on free convection heat transfer was studied by Miyamoto et al. (1980). A transformation of the boundary layer equations for free convection past a vertical plate with arbitrary blowing and wall temperature variations was studied by Vidhanayagam et al. (1980). Moreover, Raptis and Kafoussias (1982) investigated the problem of MHD free convection flow and mass transfer through a porous medium bounded by an infinite vertical porous plate with constant heat flux. Pozzi and Lupo (1988) investigated the coupling of conduction with laminar convection along a flat plate. Lin and Yu (1988) studied further detail discussion of a heated isothermal horizontal surface with transpiration.

The problem of the free convection boundary layer on a vertical plate with prescribed surface heat flux was studied by Merkin and Mahmood (1990). Hossain (1992) analyzed the viscous and Joule heating effects on MHD free convection flow with variable plate

Introduction.

temperature. Pop et al. (1995) then extended the analysis to conjugate mixed convection on a vertical surface in porous medium. Moreover, the thermal interaction between laminar film condensation and forced convection along a conducting wall was investigated by Chen and Chang (1996). Merkin and Pop (1996) analyzed the Conjugate free convection on a vertical surface. Hossain et al. (1997) studied the free convection boundary layer flow along a vertical porous plate in presence of magnetic field. Also Hossain et al. (1998) investigated the heat transfer response of MHD free convection flow along a vertical plate to surface temperature oscillation. Shu and Pop (1999) analyzed the thermal interaction between free convection and forced convection along a vertical conducting wall. Al-Khawaja et al. (1999) also studied MHD mixed convection flow

MHD free convection flow of visco-elastic fluid past an infinite porous plate was investigated by Chowdhury and Islam (2000). Elbashbeshy (2000) also discussed the effect of free convection flow with variable viscosity and thermal diffusivity along a vertical plate in the presence of magnetic field. Khan (2002) investigated the conjugate effect of conduction and convection with natural convection flow from a vertical flat plate. Ahmad and Zaidi (2004) investigated the magnetic effect on oberbeck convection through vertical stratum. Chen (2006) analyzed a numerical simulation of micropolar fluid flows along a flat plate with wall conduction and buoyancy effects. Alim et al (2007) investigated the Joule heating effect on the coupling of conduction with MHD free convection flow from a vertical flat plate. Alim et al. also studied the combined effect of viscous dissipation & Joule heating on the coupling of conduction & free convection along a vertical flat plate (2008). Rahman et al. (2008) investigated the effects of temperature dependent thermal conductivity on MHD free convection flow along a vertical flat plate with heat conduction.

In all the aforementioned analyses the effects of temperature dependent thermal conductivity with Joule heating and viscous dissipation have not been considered. In the present work, the effects of temperature dependent thermal conductivity on the coupling of conduction and Joule heating with MHD free convection flow along a vertical flat plate have been investigated. The results have been obtained for different values of relevant physical parameters. The governing partial differential equations are reduced to locally non-similarity partial differential forms by adopting appropriate transformations. The transformed boundary layer equations are solved numerically using implicit finite

Introduction.

difference method together with Keller (1978) box technique and later used by Cebeci and Bradshaw (1984).

In chapter 2, the effects of the temperature dependent thermal conductivity on the coupling of conduction and Joule heating with MHD free convection flow along a vertical flat plate have been analyzed. Velocity, temperature, skin friction coefficient and surface temperature profiles have been presented graphically for various values of the thermal conductivity variation parameter γ , magnetic parameter M , Prandtl number Pr and Joule heating parameter J . In tabular form the numerical results of the local skin friction coefficient and the surface temperature profile for different values of Joule heating parameter J are also represented. The comparisons of the present numerical results of the skin friction coefficient and the surface temperature profile with those obtained by Pozzi and Lupo (1988) and Merkin and Pop (1996) are presented.

In chapter 3, MHD natural convection flow of an electrically conducting fluid along a vertical flat plate with variable thermal conductivity on the coupling of conduction and Joule heating in presence of viscous dissipation has been described. Here numerical results of the velocity, temperature, skin friction coefficient and surface temperature profiles for different values of the viscous dissipation parameter N , thermal conductivity variation parameter γ , magnetic parameter M , Prandtl number Pr , and Joule heating parameter J have been presented graphically. Some results for skin friction coefficient and surface temperature for different values of viscous dissipation parameter have also been presented in tabular form as well. The comparison of numerical values of the skin friction coefficient for different values of thermal conductivity variation parameter (with and without the effect of viscous dissipation parameter N) is also given.

Effects of Variable Thermal Conductivity on the Coupling of Conduction and Joule Heating with Magnetohydrodynamic Free Convection Flow along a Vertical Flat Plate

2.1 Introduction

The effects of the temperature dependent thermal conductivity on MHD free convection flow along a vertical flat plate with Joule heating and conduction have been described in this chapter. The governing boundary layer equations are transformed into a non-dimensional form and the resulting non-linear system of partial differential equations is solved numerically by very efficient implicit finite-difference method together with Keller-box technique. Numerical results of velocity, temperature, skin friction coefficient and surface temperature profiles for magnetic parameter M , thermal conductivity variation parameter γ , Prandtl number Pr and Joule heating parameter J are presented graphically. Also in tabular form numerical results of skin friction coefficient and surface temperature profile are shown for Joule heating parameter J . In the following section detailed derivations of the governing equations for the flow and heat transfer and the method of solutions along with the results and discussion are presented.

2.2 Governing equations of the flow

The mathematical statement of the basic conservation laws of mass, momentum and energy for the steady two-dimensional viscous incompressible and electrically conducting flow are respectively

$$\nabla \cdot \vec{V} = 0 \tag{2.1}$$

$$\rho(\vec{V} \cdot \nabla)\vec{V} = -\nabla p + \mu \nabla^2 \vec{V} + \vec{F} + (\vec{J} \times \vec{B})_x \tag{2.2}$$

$$\rho C_p (\vec{V} \cdot \nabla) T_f = \nabla \cdot (\kappa_f \nabla T_f) + \bar{u} (\vec{J} \times \vec{V}) \tag{2.3}$$

where $\vec{V} = (\bar{u}, \bar{v})$, \bar{u} and \bar{v} are the velocity components along the \bar{x} and \bar{y} axes respectively, \vec{F} is the body force per unit volume which is defined as $-\rho g$, the terms \vec{J} and \vec{B} are respectively the current density and magnetic induction vector and the term $\vec{J} \times \vec{B}$ is the force on the fluid per unit volume produced by the interaction of current and magnetic field in the absence of excess charges. T_f is the temperature of the fluid in the

MHD free convection flow along a vertical flat plate with Joule heating

boundary layer, g is the acceleration due to gravity, κ_f is the thermal conductivity of the fluid and C_p is the specific heat at constant pressure and μ is the viscosity of the fluid. Here $\bar{B} = \mu_e H_0$, μ_e being the magnetic permeability of the fluid, H_0 is the applied magnetic field strength and ∇ is the vector differential operator and is defined by

$$\nabla = \hat{i}_x \frac{\partial}{\partial \bar{x}} + \hat{j}_y \frac{\partial}{\partial \bar{y}} \quad (2.4)$$

where \hat{i}_x and \hat{j}_y are the unit vector along \bar{x} and \bar{y} axes respectively. When the external electric conductivity of the fluid is zero and the induced electric field is negligible, the current density is related to the velocity by Ohm's law as follows

$$\bar{J} = \sigma (\bar{V} \times \bar{B}) \quad (2.5)$$

where $(\bar{V} \times \bar{B})$ is electrical fluid vector and σ denotes the electrical conductivity of the fluid under the conduction that the magnetic Reynold's number is small. This conduction is usually well satisfied in terrestrial application especially by low velocity free convection flow. So it can be written as

$$\bar{B} = \hat{j}_y H_0 \quad (2.6)$$

Bringing together equations from (2.4) to (2.6) the force per unit volume $\bar{J} \times \bar{B}$ acting along the \bar{x} -axis takes the following form

$$(\bar{J} \times \bar{B})_x = -\sigma H_0^2 \bar{u} \quad (2.7)$$

Again together equations (2.5) and (2.6) the Joule heating term in vector form becomes

$$\bar{u}(\bar{J} \times \bar{V}) = \sigma H_0^2 \bar{u}^2 \quad (2.8)$$

Consider a steady natural convection flow of an electrically conducting, viscous and incompressible fluid along a vertical flat plate of length l and thickness b (Figure-2.1). It is assumed that the temperature at the outside surface is maintained at a constant temperature T_b , where $T_b > T_\infty$, the ambient temperature of the fluid. A uniform magnetic field of strength H_0 is imposed along the \bar{y} -axis.

Using the equations (2.4) to (2.8) with respect to above considerations into the basic equations (2.1) to (2.3), the steady two dimensional laminar free convection boundary layer flow of a viscous incompressible fluid with Joule heating and also thermal

MHD free convection flow along a vertical flat plate with Joule heating

conductivity variation along a vertical flat plate takes following electrically conducting form

$$\frac{\partial \bar{u}}{\partial \bar{x}} + \frac{\partial \bar{v}}{\partial \bar{y}} = 0 \quad (2.9)$$

$$\bar{u} \frac{\partial \bar{u}}{\partial \bar{x}} + \bar{v} \frac{\partial \bar{u}}{\partial \bar{y}} = \nu \frac{\partial^2 \bar{u}}{\partial \bar{y}^2} + \kappa \beta (T_f - T_\infty) - \frac{\sigma H_0^2 \bar{u}}{\rho} \quad (2.10)$$

$$\bar{u} \frac{\partial T_f}{\partial \bar{x}} + \bar{v} \frac{\partial T_f}{\partial \bar{y}} = \frac{1}{\rho C_p} \frac{\partial}{\partial \bar{y}} \left(\kappa_f \frac{\partial T_f}{\partial \bar{y}} \right) + \frac{\sigma H_0^2 \bar{u}^2}{\rho C_p} \quad (2.11)$$

Here β is coefficient of volume expansion. Consider the temperature dependent thermal conductivity, which is proposed by Charraudeau (1975), as follows

$$\kappa_f = \kappa_\infty [1 + \delta (T_f - T_\infty)] \quad (2.12)$$

where κ_∞ is the thermal conductivity of the ambient fluid and δ is defined as

$$\delta = \frac{1}{\kappa_f} \left(\frac{\partial \kappa}{\partial T} \right)_f.$$

The appropriate boundary conditions to be satisfied by the above equations are (Merkin & Pop 1996)

$$\left. \begin{aligned} \bar{u} = 0, \quad \bar{v} = 0 \\ T_f = T(\bar{x}, 0), \quad \frac{\partial T_f}{\partial \bar{y}} = \frac{\kappa_s}{b \kappa_f} (T_f - T_b) \end{aligned} \right\} \text{ on } \bar{y} = 0, \bar{x} > 0 \quad (2.13)$$

$$\bar{u} \rightarrow 0, T_f \rightarrow T_\infty \quad \text{as } \bar{y} \rightarrow \infty, \bar{x} > 0$$

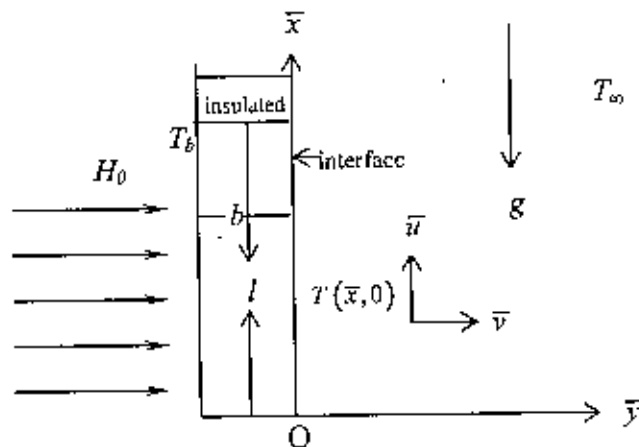


Figure 2.1: Physical model and coordinate system

It is observed that the equations (2.10) and (2.11) together with the boundary conditions (2.13) are non-linear partial differential equations. In the following sections the solution methods of these equations are discussed in details.

2.3 Transformation of the governing equations

Equations (2.9) to (2.12) will be non-dimensionalized by using the following dimensionless variables

$$x = \frac{\bar{x}}{L}, \quad y = \frac{\bar{y}}{L} Gr^{\frac{1}{4}}, \quad u = \frac{\bar{u}L}{\nu} Gr^{-\frac{1}{2}}, \quad v = \frac{\bar{v}L}{\nu} Gr^{-\frac{1}{4}}, \quad \theta = \frac{T_f - T_\infty}{T_b - T_\infty}, \quad (2.14)$$

$$Gr = \frac{g \beta L^3 (T_b - T_\infty)}{\nu^2}$$

where $L = \frac{\nu^{\frac{2}{3}}}{g^{\frac{1}{3}}}$ is reference length, Gr is the Grashof number, θ is the non dimensional

temperature, $\nu = \frac{\mu}{\rho}$ is kinematic viscosity. Substituting the relations (2.14) into the equations (2.9) to (2.11) the following non-dimensional equations are obtained

$$\frac{\partial u}{\partial x} + \frac{\partial v}{\partial y} = 0 \quad (2.15)$$

$$u \frac{\partial u}{\partial x} + v \frac{\partial u}{\partial y} + Mu = \frac{\partial^2 u}{\partial y^2} + \theta \quad (2.16)$$

$$u \frac{\partial \theta}{\partial x} + v \frac{\partial \theta}{\partial y} = \frac{1}{Pr} (1 + \gamma \theta) \frac{\partial^2 \theta}{\partial y^2} + \frac{\gamma}{Pr} \left(\frac{\partial \theta}{\partial y} \right)^2 + Ju^2 \quad (2.17)$$

where $Pr = \frac{\mu C_p}{\kappa_m}$ is the Prandtl number, $M = \frac{\sigma H_0^2 L^2}{\mu_e Gr^{1/2}}$ is the dimensionless magnetic

parameter, $\gamma = \delta(T_b - T_\infty)$ is the dimensionless thermal conductivity variation parameter

and $J = \frac{\sigma H_0^2 \nu Gr^{1/2}}{\rho C_p (T_b - T_\infty)}$ is the dimensionless Joule heating parameter. The corresponding

boundary conditions (2.13) then take the form as follows

$$u = 0, v = 0, \theta - 1 = (1 + \gamma \theta) Pr \frac{\partial \theta}{\partial y}, \quad \text{on } y = 0, x > 0 \quad (2.18)$$

$$u \rightarrow 0, \theta \rightarrow 0, \quad \text{as } y \rightarrow \infty, x > 0$$

MHD free convection flow along a vertical flat plate with Joule heating

where $p = \left(\frac{\kappa_w b}{\kappa_s L} \right) Gr^{1/4}$ is the conjugate conduction parameter. In fact, magnitude of $O(p)$ depends on b/L and $Gr^{1/4}$ being the order of unity. L is small, the term b/L becomes greater than one. For air, $\frac{\kappa_w}{\kappa_s}$ attains very small values if the plate is highly conductive. It reaches to the order of 0.1 for material such as glass. Therefore in different cases, p is different but not always a small number. In the present investigation, it is considered that $p = 1$ which is accepted for b/L of $O\left(\frac{\kappa_w}{\kappa_s}\right)$.

To solve the equations (2.16) and (2.17) subject to the boundary conditions (2.18) the following transformations are (Merkin & Pop 1996) applied

$$\begin{aligned} \psi &= x^{\frac{4}{5}}(1+x)^{-\frac{1}{20}} f(x, \eta) \\ \eta &= y x^{-\frac{1}{5}}(1+x)^{-\frac{1}{20}} \\ \theta &= x^{\frac{1}{5}}(1+x)^{-\frac{1}{5}} h(x, \eta) \end{aligned} \quad (2.19)$$

here η is the similarity variable and ψ is stream function which satisfies the continuity equation and is related to the velocity components in the usual way as $u = \frac{\partial \psi}{\partial y}$ and

$$v = -\frac{\partial \psi}{\partial x}.$$

Moreover, $h(x, \eta)$ represents the non-dimensional temperature. Then the momentum and energy equations (equations (2.16) and (2.17) respectively) are transformed to the new co-ordinate system. At first, the velocity components are expressed in terms of the new variables for this transformation. Thus the resulting equations are

$$\begin{aligned} f''' + \frac{16+15x}{20(1+x)} f f'' - \frac{6+5x}{10(1+x)} f'^2 - M x^{\frac{2}{5}}(1+x)^{\frac{1}{10}} f' \\ + h = x \left(f' \frac{\partial f'}{\partial x} - f'' \frac{\partial f}{\partial x} \right) \end{aligned} \quad (2.20)$$

$$\begin{aligned} \frac{1}{Pr} h'' + \frac{\gamma}{Pr} \left(\frac{x}{1+x} \right)^{\frac{1}{5}} h h'' + \frac{\gamma}{Pr} \left(\frac{x}{1+x} \right)^{\frac{1}{5}} h'^2 + \frac{16+15x}{20(1+x)} f h' \\ + Jx^{\frac{7}{5}}(1+x)^{\frac{1}{10}} f'^2 - \frac{1}{5(1+x)} f' h = x \left(f' \frac{\partial h}{\partial x} - h' \frac{\partial f}{\partial x} \right) \end{aligned} \quad (2.21)$$

where prime denotes partial differentiation with respect to η . The boundary conditions as mentioned in equation (2.18) are transformed into

$$f(x,0) = f'(x,0) = 0$$

$$h'(x,0) = \frac{x^{\frac{1}{5}}(1+x)^{-\frac{1}{5}}h(x,0) - 1}{(1+x)^{-\frac{1}{4}} + \gamma x^{\frac{1}{5}}(1+x)^{-\frac{9}{20}}h(x,0)} \quad (2.22)$$

$$f'(x,\infty) \rightarrow 0, h(x,\infty) \rightarrow 0$$

The set of equations (2.20) and (2.21) together with the boundary conditions (2.22) are solved by applying implicit finite-difference method with Keller-box (1978) scheme. The solution process is given in Appendix.

From the process of numerical computation, in practical point of view, it is important to calculate the values of the surface shear stress in terms of the skin friction coefficient. This can be written in the non-dimensional form as (Mamun et al 2005)

$$C_f = \frac{Gr^{-\frac{3}{4}}L^2}{\mu\nu} \tau_w \quad (2.23)$$

where $\tau_w [= \mu(\partial \bar{u}/\partial \bar{y})_{\bar{y}=0}]$ is the shearing stress. Using the new variables described in (2.14), the local skin friction co-efficient can be written as

$$C_{f,\tau} = x^{\frac{2}{5}}(1+x)^{-\frac{3}{20}}f''(x,0) \quad (2.24)$$

The numerical values of the surface temperature profile are obtained from the relation

$$\theta(x,0) = x^{\frac{1}{5}}(1+x)^{-\frac{1}{5}}h(x,0) \quad (2.25)$$

2.4 Results and Discussion

The values of the Prandtl number are considered to be 0.73, 1.73, 2.97 and 4.24. Numerical results of the velocity, temperature, skin friction coefficient and surface temperature profiles for different values of the magnetic parameter, thermal conductivity variation parameter, Joule heating parameter and Prandtl number are presented graphically.

The magnetic field acting along the horizontal direction retards the fluid velocity with $\gamma = 0.1$, $J = 0.07$ and $Pr = 0.73$ as shown in figure 2.2. Because there creates a Lorentz force by the interaction between the applied magnetic field and flow field. This force acts

against the fluid flow. From figure 2.3, it can be observed that the temperature within the boundary layer increases for the increasing values of M from 0.1 to 3.7. The magnetic field decreases the temperature gradient at the wall and increases the temperature in the flow region due to the interaction. It is also observed that the temperature at the interface varies due to the conduction within the plate.

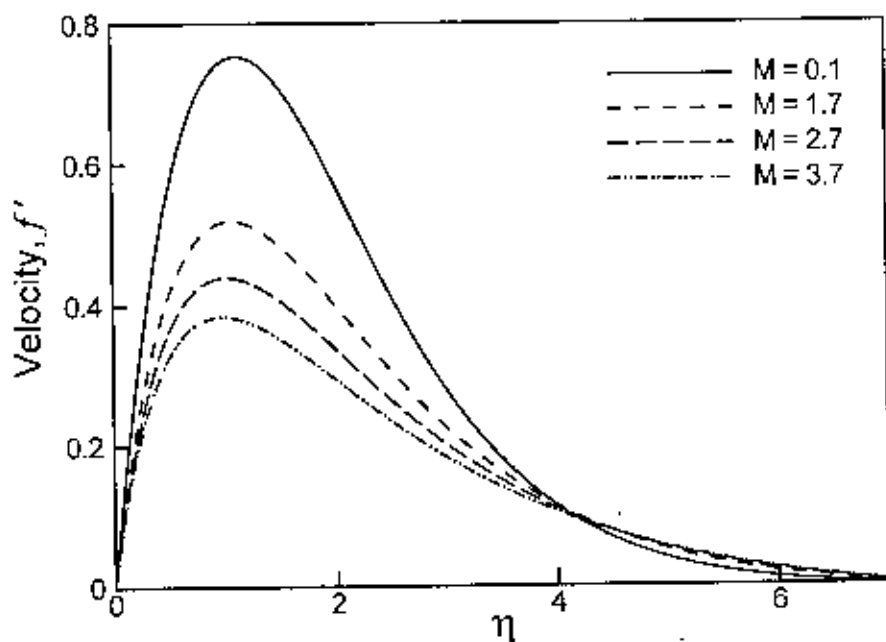


Figure 2.2: Variation of velocity profile against η for varying of M with $\gamma = 0.10, J = 0.07$ and $Pr = 0.73$

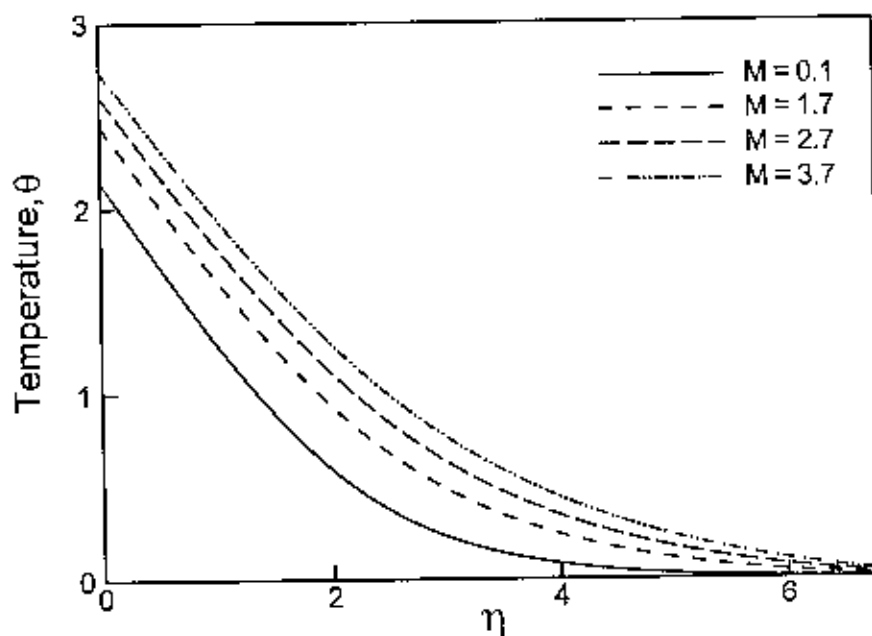


Figure 2.3: Variation of temperature profile against η for varying of M with $\gamma = 0.10, J = 0.07$ and $Pr = 0.73$.

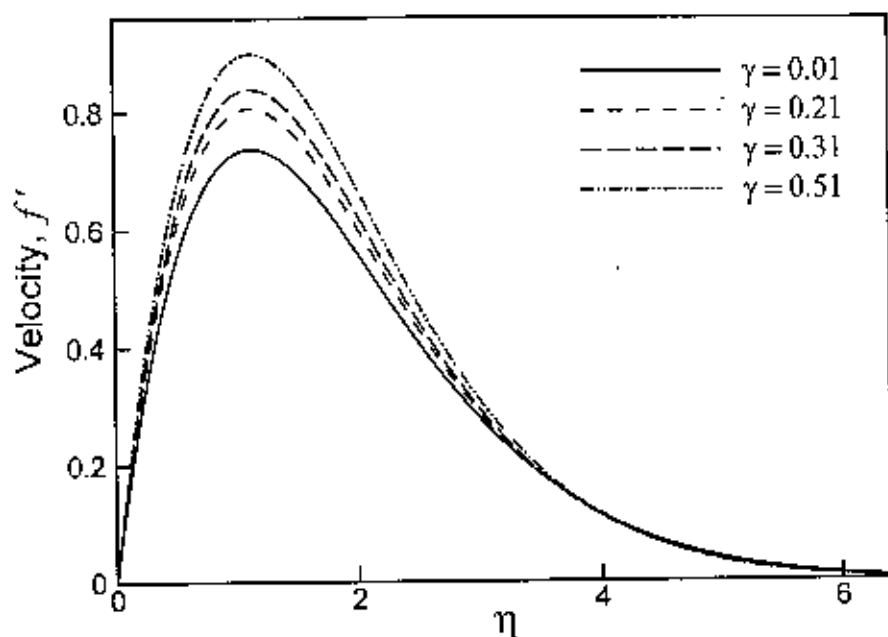


Figure 2.4: Variation of velocity profile against η for varying of γ with $M = 0.01$, $J = 0.01$ and $Pr = 0.73$

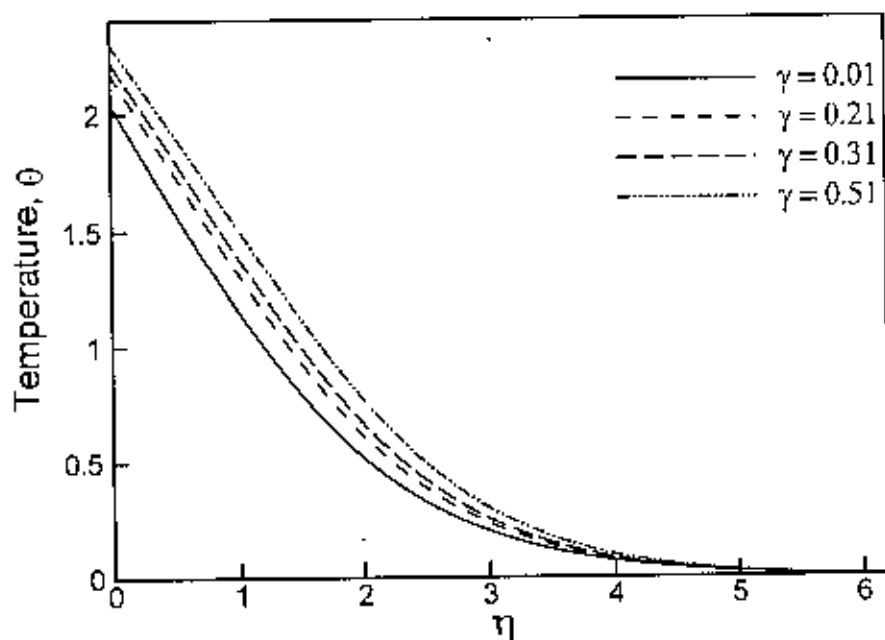


Figure 2.5: Variation of temperature profile against η for varying of γ with $M = 0.01$, $J = 0.01$ and $Pr = 0.73$

The effect of thermal conductivity variation parameter γ on velocity and temperature profiles within the boundary layer with other fixed parameters $M = 0.01$, $J = 0.01$ and $Pr =$

0.73 are shown in figure 2.4 and figure 2.5, respectively. As $\gamma = \delta(T_b - T_\infty)$, so increasing values of γ increase this temperature difference between outside the plate and outside boundary layer. Then heat is transferred rapidly from plate to fluid within the boundary layer. That's why both velocity and temperature profiles increase with the increasing values of γ . Moreover, the maximum values of the velocity are 0.7371, 0.8069, 0.8396 and 0.9001 for $\gamma = 0.01, 0.21, 0.31$ and 0.51 , respectively and each of which occurs at $\eta = 1.1144$. It is observed that the velocity increases by 18.11% when γ increases from 0.01 to 0.51. Furthermore, the maximum values of the temperature are 2.0446, 2.1735, 2.2225 and 2.2972 for $\gamma = 0.01, 0.21, 0.31$, and 0.51 , respectively. Each of which occurs at the surface because thermal conductivity of solid is greater than fluid. It is observed that the temperature increases by 10.996% when γ increases from 0.01 to 0.51.

Figure 2.6 and figure 2.7 illustrate the velocity and temperature profiles for different values of Prandtl number Pr with $M = 0.10, J = 0.07$ and $\gamma = 0.10$. It is well known that Prandtl number is the ratio of viscous force and thermal force. So, increasing values of Pr increase viscosity and decreases thermal action of the fluid. If viscosity is increased, then fluid does not move freely. Because of this fact, it can be observed from figure 2.6 that the velocity decreases as well as its position moves toward the interface with the increasing Prandtl number. Also from figure 2.7, it is seen that the temperature profile shift downward with the increasing Pr . It is shown that the velocity decreases by 52.45% when Pr increases from 0.73 to 4.24. Furthermore, the temperature decreases by 30.37% for increasing values of Pr at the interface.

The effect of Joule heating parameter J on the velocity and the temperature profiles within the boundary layer with $M = 0.01, \gamma = 0.01$ and $Pr = 0.73$ are shown in figure 2.8 and figure 2.9 respectively. Due to Joule heating effect, temperature of the conductor increases and electrical energy is transferred to thermal energy. So increasing values of J increases temperature of the plate and temperature difference of $(T_b - T_\infty)$. Then velocity, as well as temperature profile increases within the boundary layer with the increasing value of J . Moreover, the maximum values of the velocity are 0.7354, 0.7476, 0.7565 and 0.7723 for $J = 0.001, 0.15, 0.27$ and 0.48 respectively and each of which occurs at $\eta = 1.1144$. It is observed that the velocity increases by 4.78% when J increases from 0.001 to 0.48. Furthermore, the maximum values of the temperature are 2.0424, 2.0782, 2.1077 and 2.1608 for $J = 0.001, 0.150, 0.270$, and 0.480 respectively and each of which occurs at the

surface. It is observed that the temperature increases by 5.48% when J increases from 0.001 to 0.480.

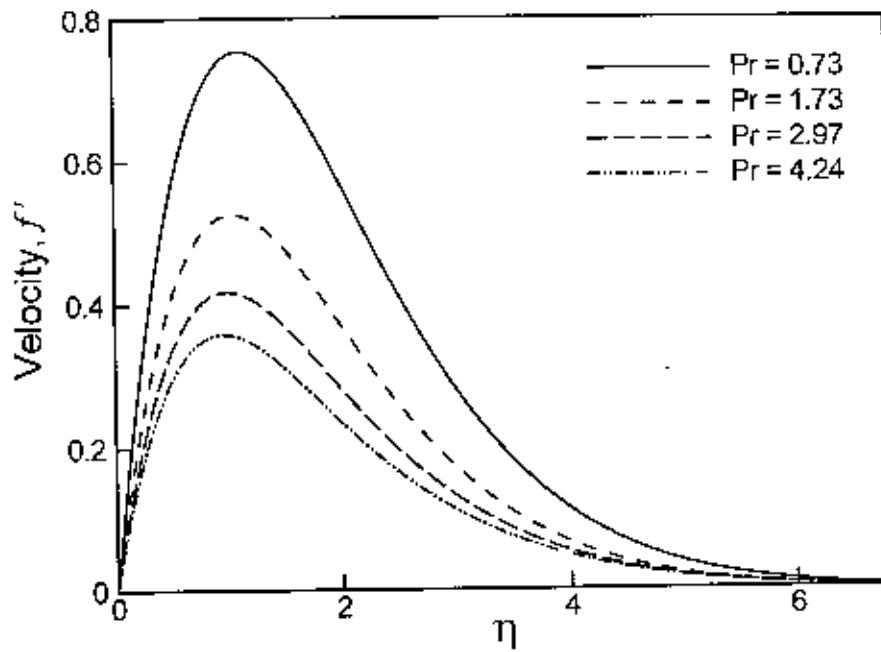


Figure 2.6: Variation of velocity profile against η for varying of Pr with $M = 0.10$, $J = 0.07$ and $\gamma = 0.10$

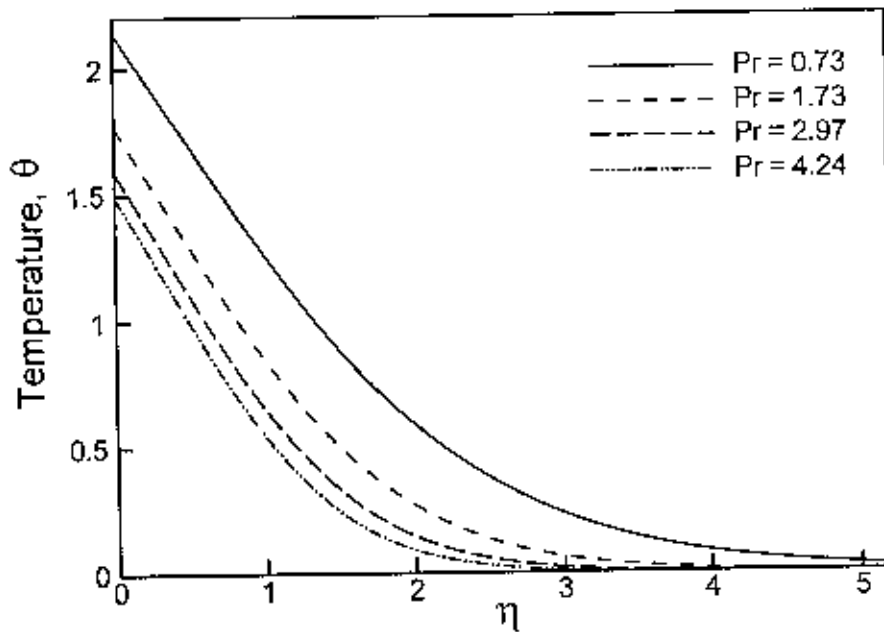


Figure 2.7: Variation of temperature profile against η for varying of Pr with $M = 0.10$, $J = 0.07$ and $\gamma = 0.10$

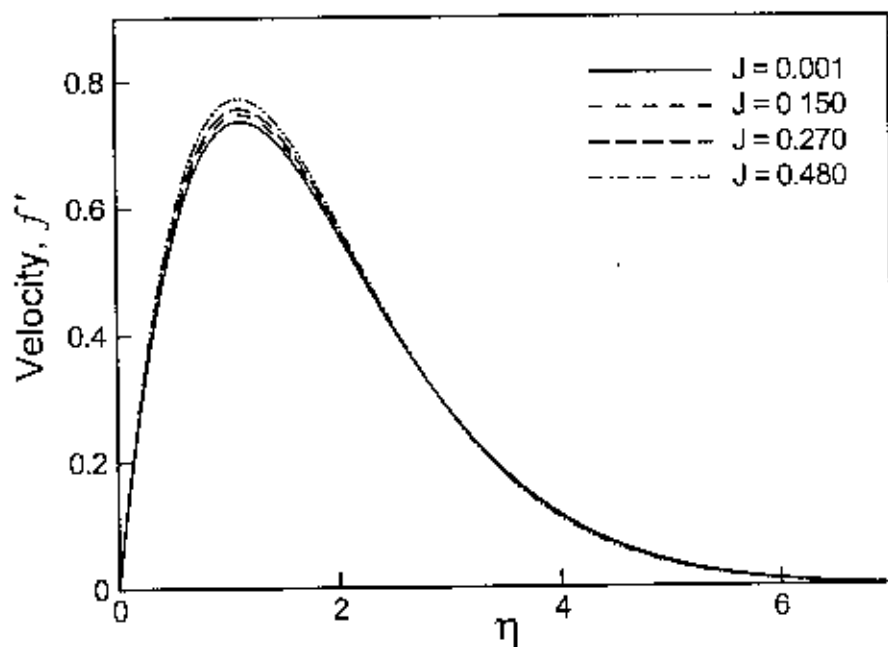


Figure 2.8: Variation of velocity profile against η for varying of J with $\gamma = 0.01$, $M = 0.01$ and $Pr = 0.73$

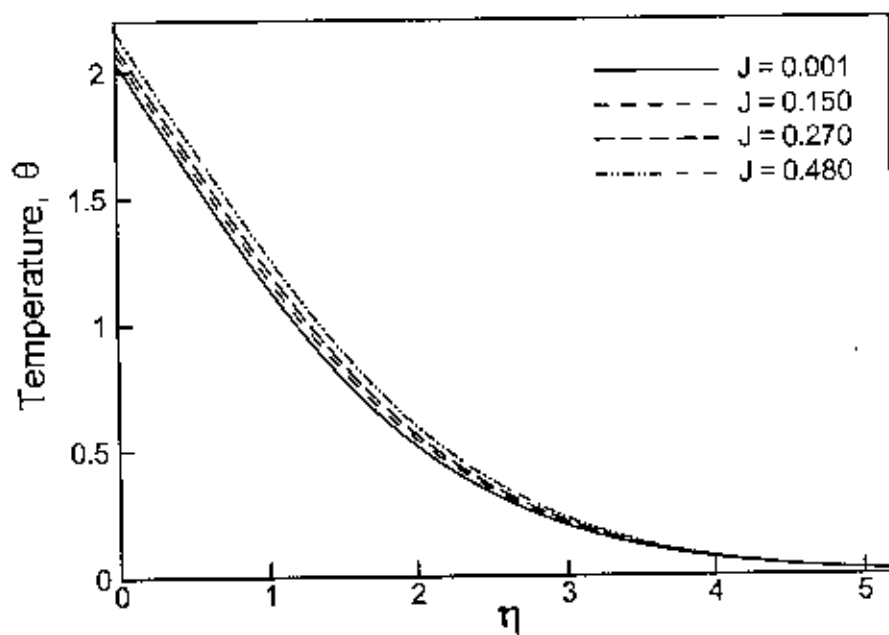


Figure 2.9: Variation of temperature profile against η for varying of J with $\gamma = 0.01$, $M = 0.01$ and $Pr = 0.73$

The variation of the local skin friction coefficient C_{fx} and surface temperature profile $\theta(x,0)$ for different values of M with $Pr = 0.73$, $J = 0.07$ and $\gamma = 0.10$ at different positions are illustrated in figure 2.10 and figure 2.11 respectively. It is observed from figure 2.10 that the increased value of the Magnetic parameter M leads to a decrease of the skin friction factor. Again figure 2.11 shows that the surface temperature $\theta(x,0)$ increases due to the increasing values of M . This is due to the interaction between magnetic field and flow field. It can also be noted that the surface temperature increases along the up ward direction of the plate for a particular value of M . The magnetic field acts against the fluid flow and reduces the skin friction coefficient and produces the temperature at the solid-fluid interface.

Figure 2.12 and figure 2.13 illustrate the effects of the thermal conductivity variation parameter on the skin friction coefficient and surface temperature profile against x with $M = 0.01$, $J = 0.01$ and $Pr = 0.73$. It is seen that the skin friction coefficient increases monotonically along the up ward direction of the plate for a particular value of γ . It is also shown that the skin friction coefficient increases for the increasing γ . The same result is observed for the surface temperature from figure 2.13. This is to be expected because the higher value for the thermal conductivity variation parameter accelerates the fluid flow and increases the temperature as mentioned in figure 2.4 and figure 2.5 respectively.

Figure 2.14 and figure 2.15 deal with the effects of Prandtl number on the skin friction coefficient and surface temperature profile against x with $M = 0.10$, $J = 0.07$ and $\gamma = 0.10$. It can be observed from figure 2.14 that the skin friction coefficient increases monotonically for a particular value of Pr . It is also noted that the skin friction coefficient decreases for the increasing Prandtl number. From figure 2.15, it can be seen that the surface temperature decreases due to the increasing values of Pr from 0.73 to 4.24.

Figure 2.16 and figure 2.17 deal with the effect of Joule heating parameter on the skin friction coefficient and surface temperature profile against x with $M = 0.01$, $Pr = 0.73$ and $\gamma = 0.01$. It can be observed from figure 2.16 that the skin friction coefficient increases monotonically for a particular value of J . It can also be noted that the skin friction coefficient increases for the increasing J . From figure 2.17, it can be seen that the surface temperature increases due to the increasing values of J from 0.001 to 0.480

In this problem the values of parameters (magnetic parameter $M = 0.1, 1.7, 2.7, 3.7$, thermal conductivity variation parameter $\gamma = 0.01, 0.21, 0.31, 0.51$, Joule heating parameter $J = 0.001, 0.150, 0.270, 0.480$, and Prandtl number $Pr = 0.73, 1.73, 2.97, 4.24$)

are taken. It is observed that for each parameter, if greater than above value is taken then it does not converge with other controlling parameters. In that case figures of velocity, temperature, skin friction coefficient and surface temperature profiles will not be better than that are shown above. Also then the fluid flow will no longer be laminar.

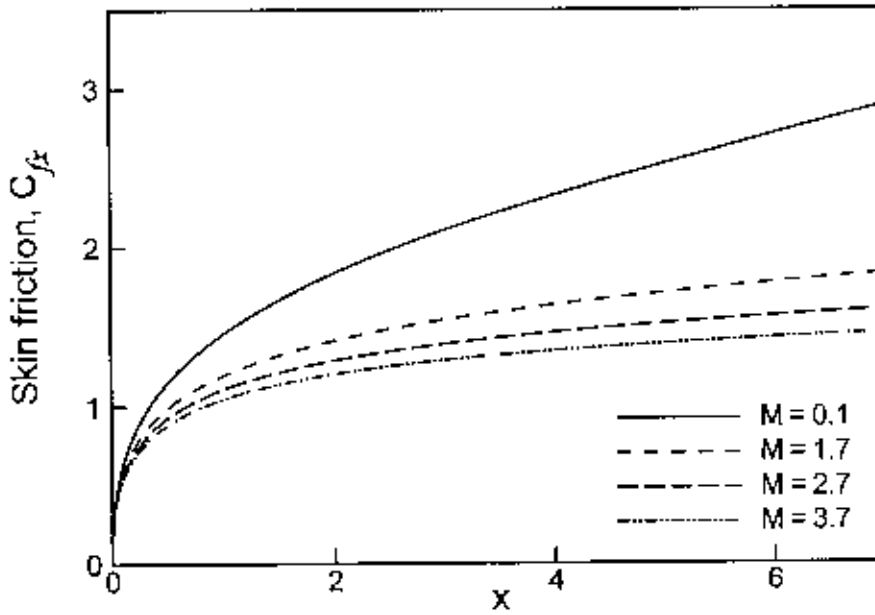


Figure 2.10: Variation of skin friction coefficient against x for varying of M with $\gamma = 0.1$, $J = 0.07$ and $Pr = 0.73$

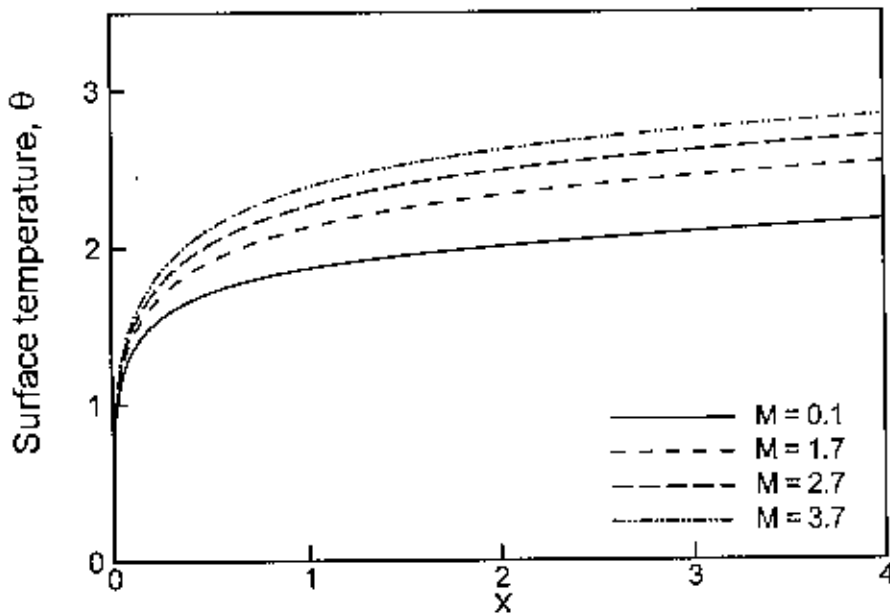


Figure 2.11: Variation of surface temperature profile against x for varying of M with $\gamma = 0.1$, $J = 0.07$ and $Pr = 0.73$

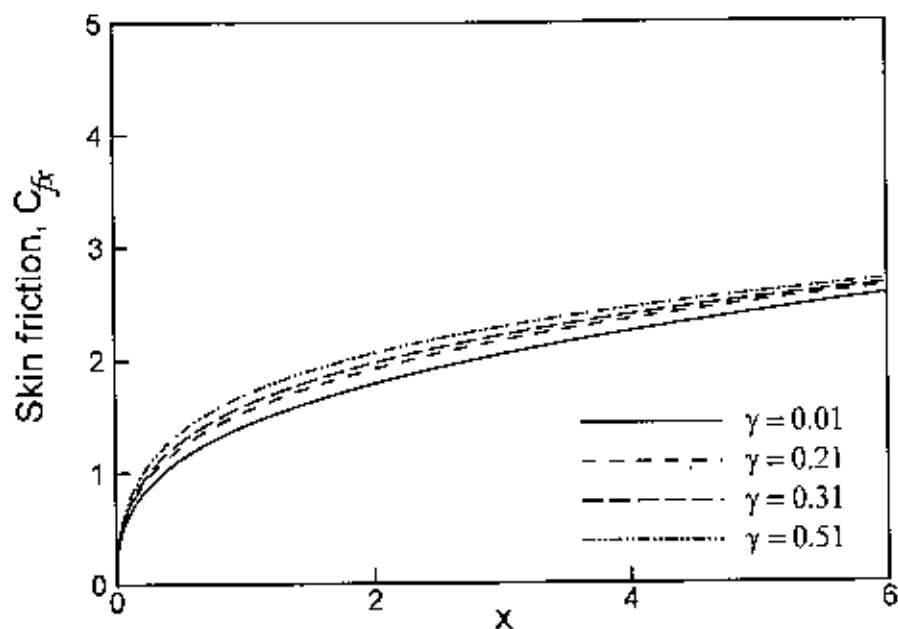


Figure 2.12: Variation of skin friction coefficient against x for varying of γ with $M = 0.01$, $J = 0.01$ and $Pr = 0.73$

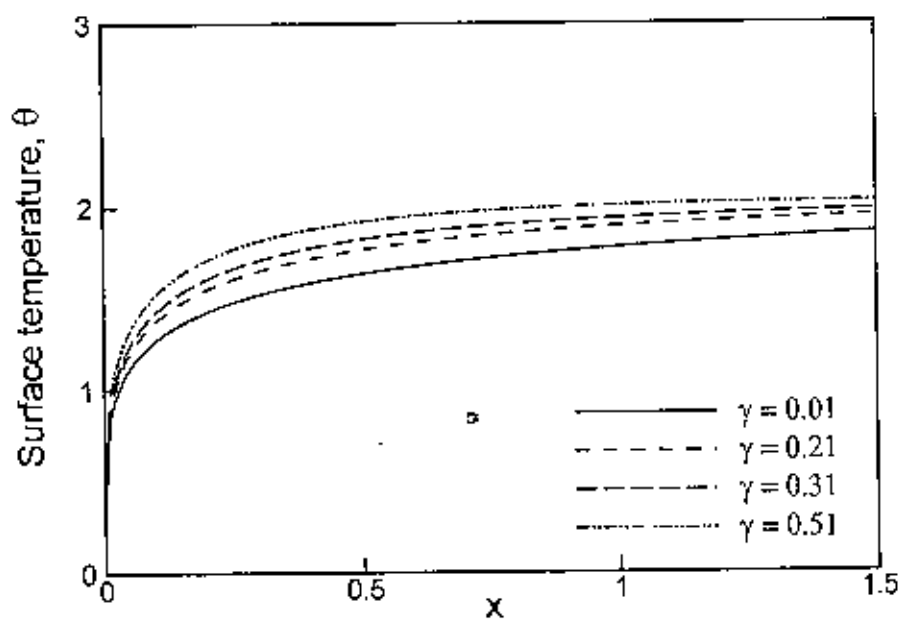


Figure 2.13: Variation of surface temperature profile against x for varying of γ with $M = 0.01$, $J = 0.01$ and $Pr = 0.73$

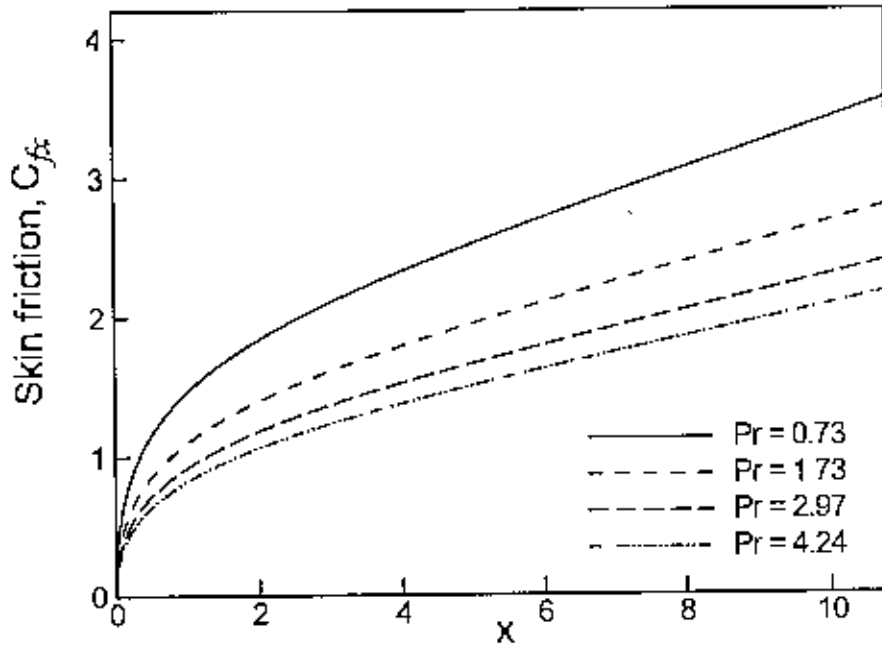


Figure 2.14: Variation of skin friction coefficient against x for varying of Pr with $M = 0.10$, $J = 0.07$ and $\gamma = 0.10$

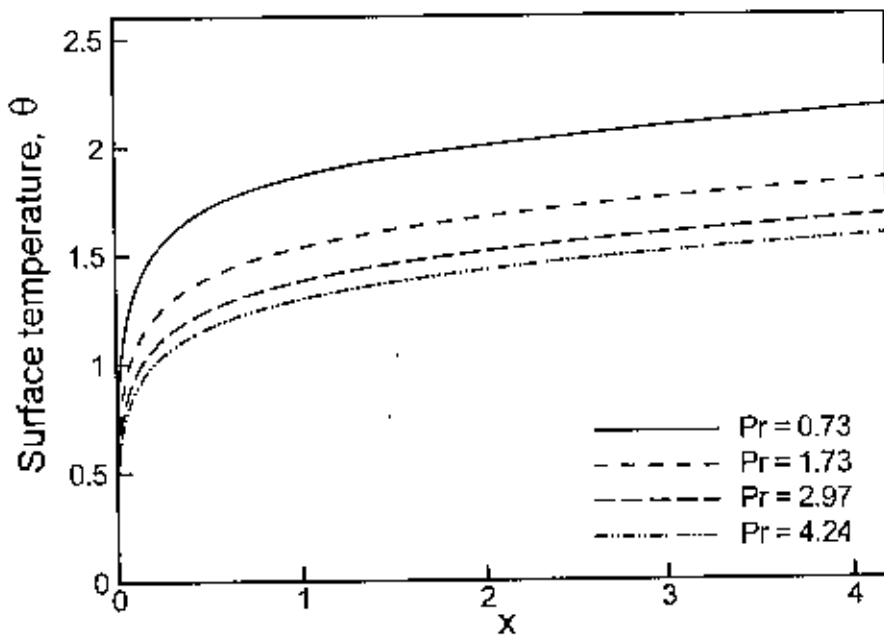


Figure 2.15: Variation of surface temperature profile against x for varying of Pr with $M = 0.10$, $J = 0.07$ and $\gamma = 0.10$

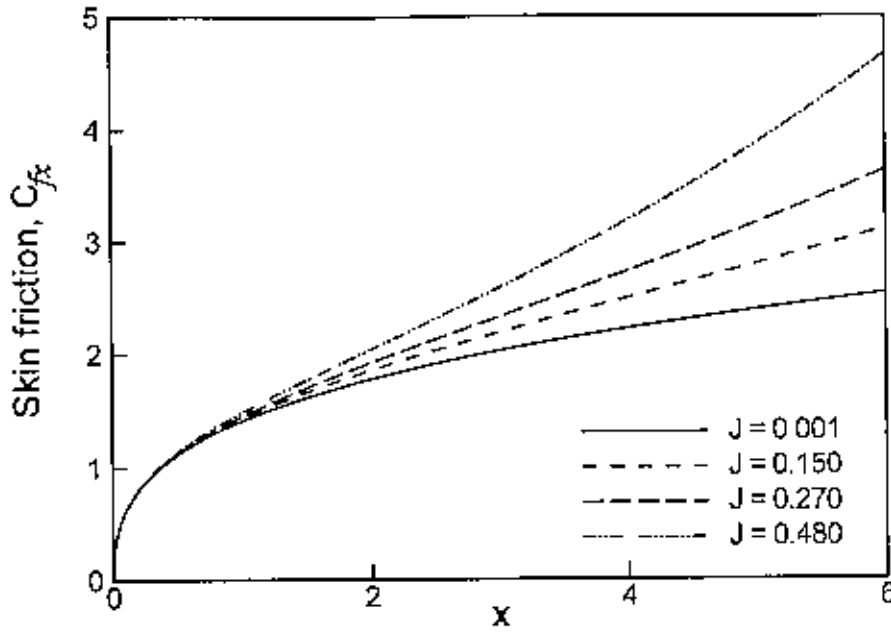


Figure 2.16: Variation of skin friction coefficient against x for varying of J with $M=0.01$, $\gamma=0.01$ and $Pr=0.73$

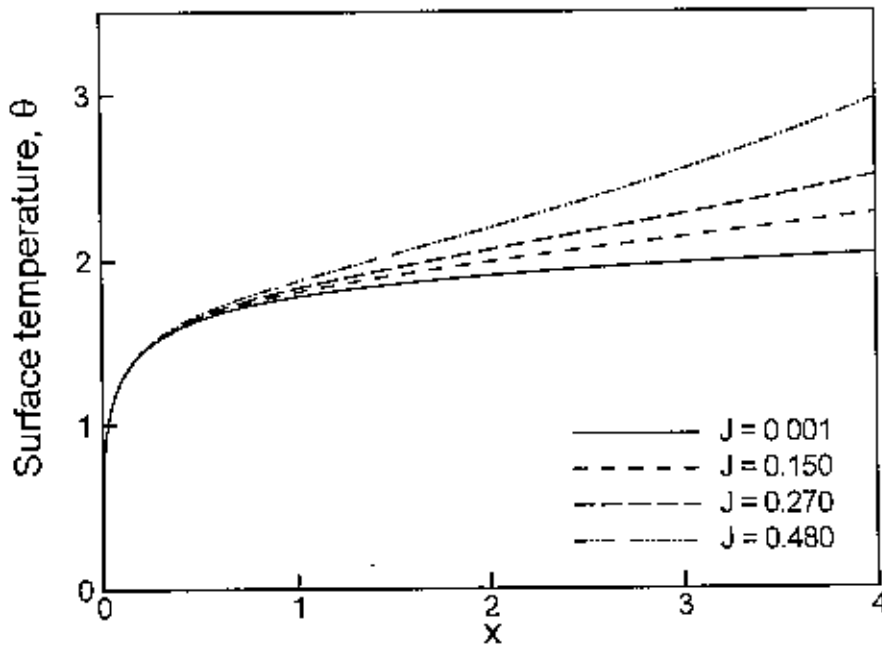


Figure 2.17: Variation of surface temperature profile against x for varying of J with $M=0.01$, $\gamma=0.01$ and $Pr=0.73$

Table 2.2 and 2.3 depict the comparisons of the present numerical results of the surface temperature $\theta(x,0)$ and the skin friction coefficient C_{f_x} with those obtained by Pozzi and Lupo (1988) and Merkin and Pop (1996) respectively.

MHD free convection flow along a vertical flat plate with Joule heating

Here, the magnetic parameter M , thermal conductivity variation parameter γ and Joule heating parameter J are ignored and the Prandtl number $Pr = 0.733$ with $x^{1/5} = \xi$ is chosen. It is clearly seen that there is an excellent agreement of the present results with the solutions of Pozzi and Lupo in 1988 and Merkin and Pop in 1996.

Table 2.1: Comparison of the present numerical results of surface temperature profile with Prandtl number $Pr = 0.733$, $M = 0.0$, $J = 0.0$ and $\gamma = 0.0$

$\theta(x,0)$			
$\frac{1}{x^5} = \xi$	Pozzi and Lupo (1988)	Merkin and Pop (1996)	Present work
0.7	0.651	0.651	0.651
0.8	0.684	0.686	0.687
0.9	0.708	0.715	0.717
1.0	0.717	0.741	0.741
1.1	0.699	0.762	0.763
1.2	0.640	0.781	0.781

Table 2.2: Comparison of the present numerical results of skin friction coefficient with Prandtl number $Pr = 0.733$, $M = 0.0$, $J = 0.0$ and $\gamma = 0.0$

C_f			
$\frac{1}{x^5} = \xi$	Pozzi and Lupo (1988)	Merkin and Pop (1996)	Present work
0.7	0.430	0.430	0.424
0.8	0.530	0.530	0.528
0.9	0.635	0.635	0.634
1.0	0.741	0.745	0.743
1.1	0.829	0.859	0.858
1.2	0.817	0.972	0.973

Table 2.3: Skin friction coefficient and surface temperature profile against x for different values of Joule heating parameter J with other controlling parameters $\gamma = 0.01$, $M = 0.01$ and $Pr = 0.73$

x	$J=0.001$		$J=0.150$		$J=0.270$		$J=0.480$	
	C_{fx}	θ	C_{fx}	θ	C_{fx}	θ	C_{fx}	θ
0.8881	1.3558	1.7538	1.3744	1.7779	1.3895	1.7976	1.4163	1.8329
1.3356	1.5560	1.8323	1.5943	1.8772	1.6258	1.9145	1.6820	1.9824
2.5346	1.9202	1.9504	2.0398	2.0702	2.1406	2.1746	2.3260	2.3742
3.7803	2.1846	2.0246	2.4298	2.2489	2.6427	2.4553	3.0461	2.8718
4.9370	2.3802	2.0757	2.7786	2.4209	3.1348	2.7555	3.8260	3.4635
5.5785	2.4753	2.0996	2.9741	2.5220	3.4272	2.9436	4.3167	3.8572
6.6947	2.6245	2.1361	3.3246	2.7112	3.9777	3.3143	5.2829	4.6713
7.8683	2.7641	2.1691	3.7135	2.9314	4.6226	3.7715	6.4673	5.7276
8.7021	2.8549	2.1900	4.0056	3.1030	5.1268	4.1436	7.4224	6.6187
9.2437	2.9108	2.2027	4.2033	3.2219	5.4761	4.4081	8.0959	7.2657

2.5 Conclusion

From the present investigation the following conclusion may be drawn

- The velocity profile within the boundary layer increases for decreasing values of the magnetic parameter M , Prandtl number Pr and increasing values of the thermal conductivity variation parameter γ and Joule heating parameter J .
- The temperature profile within the boundary layer increases for the increasing values of M , γ and J , and decreasing values of the Prandtl number Pr .
- The skin friction coefficient decreases for the increasing value of the magnetic parameter M , Prandtl number Pr and decreasing values of the thermal conductivity variation parameter γ and Joule heating parameter J .
- An increase in the values of the thermal conductivity variation parameter γ , Joule heating parameter J and magnetic parameter M leads to increase in the surface temperature profile
- The surface temperature profile decreases for the increasing values of the Prandtl number Pr .

Combined Effects of Variable Thermal Conductivity and Joule Heating on MHD Free Convection Flow along a Vertical Flat Plate with Conduction and Viscous Dissipation.

3.1 Introduction

This chapter describes combined effects of variable thermal conductivity and Joule heating on MHD free convection flow along a vertical flat plate with heat conduction and viscous dissipation. The governing equations are made dimensionless by using a new class of transformations. The resulting non-linear system of partial differential equations is then solved numerically using very efficient implicit finite-difference method known as Keller-box scheme. Numerical results are presented graphically by velocity, temperature, skin friction coefficient and surface temperature profiles for a selection of parameters set consisting of magnetic parameter M , thermal conductivity variation parameter γ , viscous dissipation parameter N , Joule heating parameter J and Prandtl number Pr . The comparison of numerical values of the skin friction coefficient for different values of thermal conductivity variation parameter (with and without the effect of viscous dissipation parameter N) is also given as well.

3.2 Governing equations of the flow

In the present work it is assumed that a steady natural convection flow of an electrically conducting, viscous and incompressible fluid along a vertical flat plate of length l and thickness b (Figure-3.1) The temperature at the outside surface is considered at a constant temperature T_b , where $T_b > T_\infty$ the temperature outside the boundary layer. Along the \bar{y} -axis a uniform magnetic field of strength H_0 is applied.

Under the usual Boussinesq approximation, the continuity, momentum and energy equations for two dimensional laminar flow can be written as

$$\frac{\partial \bar{u}}{\partial \bar{x}} + \frac{\partial \bar{v}}{\partial \bar{y}} = 0 \quad (3.1)$$

$$\bar{u} \frac{\partial \bar{u}}{\partial \bar{x}} + \bar{v} \frac{\partial \bar{u}}{\partial \bar{y}} = \nu \frac{\partial^2 \bar{u}}{\partial \bar{y}^2} + g\beta(T_f - T_\infty) - \frac{\sigma H_0^2 \bar{u}}{\rho} \quad (3.2)$$

$$\bar{u} \frac{\partial T_f}{\partial \bar{x}} + \bar{v} \frac{\partial T_f}{\partial \bar{y}} = \frac{1}{\rho C_p} \frac{\partial}{\partial \bar{y}} \left(\kappa_f \frac{\partial T_f}{\partial \bar{y}} \right) + \frac{\sigma H_0^2}{\rho C_p} \bar{u}^2 + \frac{\nu}{C_p} \left(\frac{\partial \bar{u}}{\partial \bar{y}} \right)^2 \quad (3.3)$$

Here β is coefficient of volume expansion. Consider the temperature dependent thermal conductivity, which is proposed by Charrardeau (1975)

$$\kappa_f = \kappa_\infty [1 + \delta(T_f - T_\infty)] \quad (3.4)$$

where κ_∞ is the thermal conductivity of the ambient fluid and δ is defined as

$$\delta = \frac{1}{\kappa_f} \left(\frac{\partial \kappa}{\partial T} \right)_f$$

The above equations are satisfied by the following appropriate boundary conditions (Merkin & Pop 1996).

$$\left. \begin{aligned} \bar{u} = 0, \quad \bar{v} = 0 \\ T_f = T(\bar{x}, 0), \quad \frac{\partial T_f}{\partial \bar{y}} = \frac{\kappa_s}{b\kappa_f} (T_f - T_b) \end{aligned} \right\} \text{ on } \bar{y} = 0, \bar{x} > 0 \quad (3.5)$$

$$\bar{u} \rightarrow 0, T_f \rightarrow T_\infty \quad \text{as } \bar{y} \rightarrow \infty, \bar{x} > 0$$

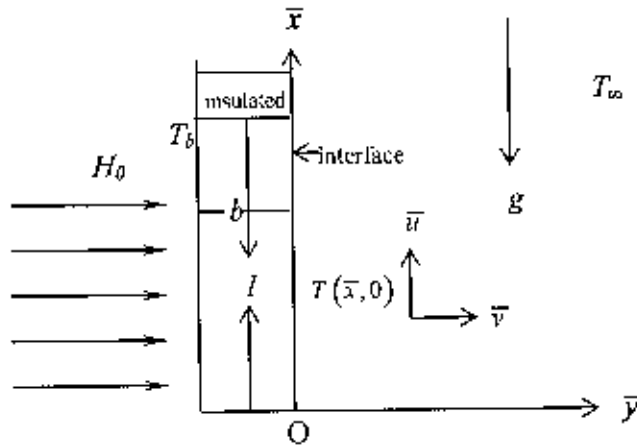


Figure 3.1: Physical model and coordinate system

3.3 Transformation of the governing equations

- The non-dimensional governing equations and boundary conditions can be obtained from equation (3.1) - (3.5) using the following non-dimensional quantities:

$$x = \frac{\bar{x}}{L}, y = \frac{\bar{y}}{L} Gr^{\frac{1}{4}}, u = \frac{\bar{u}L}{\nu} Gr^{-\frac{1}{2}}, v = \frac{\bar{v}L}{\nu} Gr^{-\frac{1}{4}}, \theta = \frac{T_f - T_\infty}{T_b - T_\infty},$$

$$Gr = \frac{g\beta L^3(T_b - T_\infty)}{\nu^2} \quad (3.6)$$

where Gr is the Grashof number, L is the reference length of the plate, θ is the non-dimensional temperature, $\nu = \frac{\mu}{\rho}$ is kinematic viscosity. Now substituting the equation

(3.6) into the equations (3.1) - (3.3), the following non-dimensional equations are obtained

$$\frac{\partial u}{\partial x} + \frac{\partial v}{\partial y} = 0 \quad (3.7)$$

$$u \frac{\partial u}{\partial x} + v \frac{\partial u}{\partial y} + Mu = \frac{\partial^2 u}{\partial y^2} + \theta \quad (3.8)$$

$$u \frac{\partial \theta}{\partial x} + v \frac{\partial \theta}{\partial y} = \frac{1}{Pr} (1 + \gamma \theta) \frac{\partial^2 \theta}{\partial y^2} + \frac{\gamma}{Pr} \left(\frac{\partial \theta}{\partial y} \right)^2 + Ju^2 + N \left(\frac{\partial u}{\partial y} \right)^2 \quad (3.9)$$

where $M = \frac{\sigma H_0^2 L^2}{\mu_e Gr^{1/2}}$ is the dimensionless magnetic parameter, $Pr = \frac{\mu C_p}{\kappa_w}$ is the Prandtl number, $\gamma = \delta(T_b - T_\infty)$ is the dimensionless thermal conductivity variation parameter,

$J = \frac{\sigma H_0^2 \nu Gr^{1/2}}{\rho C_p (T_b - T_\infty)}$ is dimensionless Joule heating parameter and $N = \frac{\nu^2 Gr}{L^2 C_p (T_b - T_\infty)}$ is

the dimensionless viscous dissipation parameter. The corresponding boundary conditions (3.5) then take the following form

$$u = 0, v = 0, \theta - 1 = (1 + \gamma \theta) p \frac{\partial \theta}{\partial y}, \text{ on } y = 0, x > 0 \quad (3.10)$$

$$u \rightarrow 0, \theta \rightarrow 0, \text{ as } y \rightarrow \infty, x > 0$$

where the conjugate conduction parameter $p = \left(\frac{\kappa_a b}{\kappa_s L} \right) Gr^{1/4}$. Magnitude of $O(p)$ depends

on b/L and $Gr^{1/4}$ being the order of unity. $\frac{\kappa_a}{\kappa_s}$ attains very small values if the plate is

highly conductive and reaches the order of 0.1 for materials such as glass. Since L is small, the term b/L becomes greater than one. p may be different in different cases but not always a small number. $p = 1$ is considered in the present investigation.

The following transformations are introduced to solve the equations (3.8) and (3.9) subject to the boundary conditions (3.10),

$$\begin{aligned} \psi &= x^{\frac{4}{3}}(1+x)^{-\frac{1}{20}} f(x, \eta) \\ \eta &= y x^{-\frac{1}{3}}(1+x)^{-\frac{1}{20}} \\ \theta &= x^{\frac{1}{3}}(1+x)^{-\frac{1}{5}} h(x, \eta) \end{aligned} \quad (3.11)$$

here ψ is stream function which satisfies the continuity equation and is related to the velocity components in the usual way as $u = \frac{\partial \psi}{\partial y}$ and $v = -\frac{\partial \psi}{\partial x}$, η is the similarity variable. Moreover, $h(x, \eta)$ represents the non-dimensional temperature. The momentum and energy equations (equation (3.8) and (3.9) respectively) are transformed for the new coordinate system. At first, the velocity components are expressed in terms of the new variables for this transformation. Thus the following equations are obtained

$$\begin{aligned} f''' + \frac{16+15x}{20(1+x)} f f'' - \frac{6+5x}{10(1+x)} f'^2 - M x^{\frac{2}{3}}(1+x)^{\frac{1}{10}} f' \\ + h = x \left(f' \frac{\partial f'}{\partial x} - f'' \frac{\partial f}{\partial x} \right) \end{aligned} \quad (3.12)$$

$$\begin{aligned} \frac{1}{Pr} h'' + \frac{\gamma}{Pr} \left(\frac{x}{1+x} \right)^{\frac{1}{5}} h h'' + \frac{\gamma}{Pr} \left(\frac{x}{1+x} \right)^{\frac{1}{5}} h'^2 + \frac{16+15x}{20(1+x)} f h' \\ + Jx^{\frac{2}{3}}(1+x)^{\frac{1}{10}} f'^2 - \frac{1}{5(1+x)} f' h + Nx f'^2 = x \left(f' \frac{\partial h}{\partial x} - h' \frac{\partial f}{\partial x} \right) \end{aligned} \quad (3.13)$$

where prime denotes partial differentiation with respect to η . The boundary conditions as mentioned in equation (3.10) then take the following form

$$\begin{aligned} f(x, 0) = f'(x, 0) = 0 \\ h'(x, 0) = \frac{x^{\frac{1}{3}}(1+x)^{-\frac{1}{5}} h(x, 0) - 1}{(1+x)^{-\frac{1}{4}} + \gamma x^{\frac{1}{3}}(1+x)^{-\frac{9}{20}} h(x, 0)} \end{aligned} \quad (3.14)$$

$$f'(x, \infty) \rightarrow 0, h(x, \infty) \rightarrow 0$$

By applying implicit finite difference method with Keller-box (1978) scheme the set of equations (3.12) and (3.13) together with the boundary conditions (3.14) can be solved.

3.4 Results and Discussion

The main objective of the present work is to analyze the combined effects of thermal conductivity variation due to temperature and Joule heating on MHD free convection flow along a vertical flat plate with heat conduction and viscous dissipation. The values of the Prandtl number are considered to be 0.73, 1.73, 2.97 and 4.24 that corresponds to air, water, methyl chloride and sulfur dioxide respectively. Detailed numerical results of the velocity, temperature, skin friction coefficient and surface temperature profiles for different values of the thermal conductivity variation parameter, viscous dissipation parameter, Joule heating parameter and Prandtl number are presented graphically. The velocity and the temperature fields obtained from the solutions of the equations (3.12) and (3.13) are depicted in figure 3.2 to figure 3.11.

Figure 3.2 and figure 3.3 illustrate the velocity and temperature profiles for different values of Prandtl number Pr with other controlling parameters $M = 0.02$, $N = 0.02$, $J = 0.01$ and $\gamma = 0.1$. From figure 3.2, it can be observed that the velocity profile decreases as well as its position moves toward the interface with the increasing Pr . From figure 3.3, it is seen that the temperature profile shifts down ward with the increasing Pr .

The effect of viscous dissipation parameter N on the velocity and the temperature within the boundary layer with $M = 2.6$, $\gamma = 0.02$, $J = 0.01$ and $Pr = 0.73$ are shown in figure 3.4 and figure 3.5 respectively. The velocity and temperature increase within the boundary layer with the increasing values of N . Moreover, the maximum values of the velocity are 0.2701, 0.2777, 0.2860 and 0.3007 for $N = 0.01, 0.50, 1.00$ and 1.80 respectively and each of which occurs at $\eta = 1.1412$. It is observed that the velocity increases by 10.18 % when N increases from 0.01 to 1.80. Furthermore, the maximum values of the temperature are 0.9133, 0.9395, 0.9693 and 1.0250 for $N = 0.01, 0.50, 1.00$, and 1.80 respectively and each of which occurs at the surface. It is observed that the temperature increases by 10.9 % when N increases from 0.01 to 1.80

Figure 3.6 and 3.7 show the effect of Joule heating parameter J on the velocity and temperature profiles within the boundary layer with other controlling parameters $M = 2.6$, $\gamma = 0.01$, $N = 0.01$ and $Pr = 1.73$ respectively. It is seen that from figure 3.6 and figure 3.7 that these profiles increase within the boundary layer with the increasing values of J from 0.01 to 0.23.

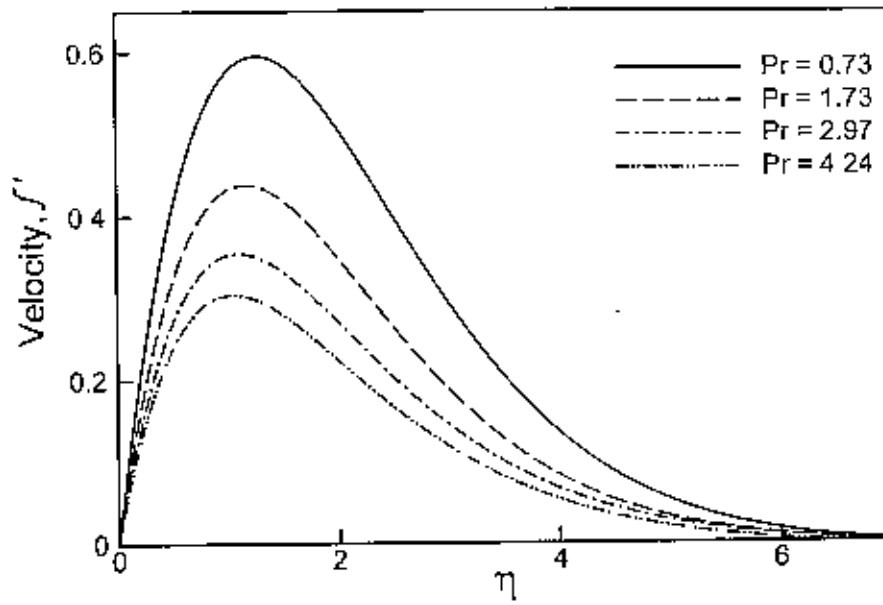


Figure 3.2: Variation of velocity profile against η for varying of Pr with $M = 0.02$, $N = 0.02$, $J = 0.01$ and $\gamma = 0.1$

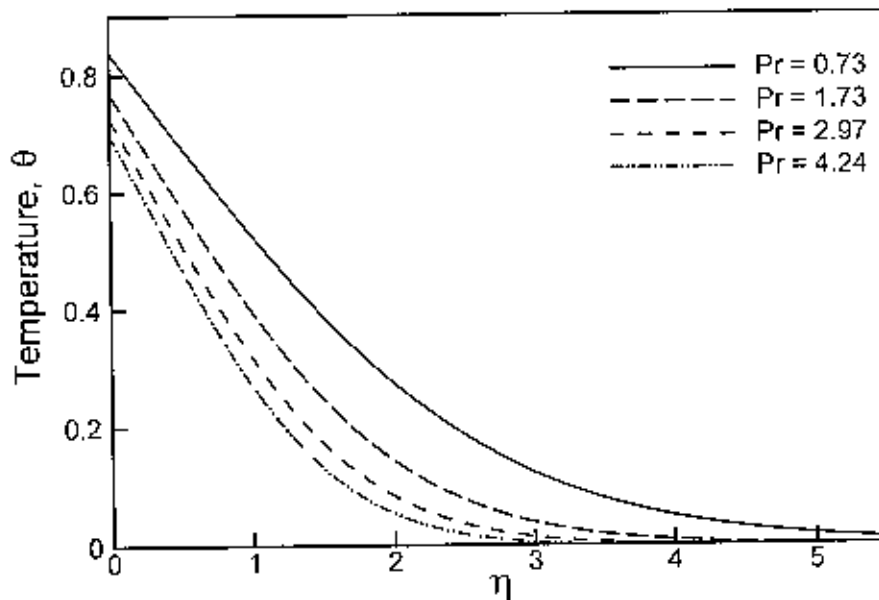


Figure 3.3: Variation of temperature profile against η for varying of Pr with $M = 0.02$, $N = 0.02$, $J = 0.01$ and $\gamma = 0.1$

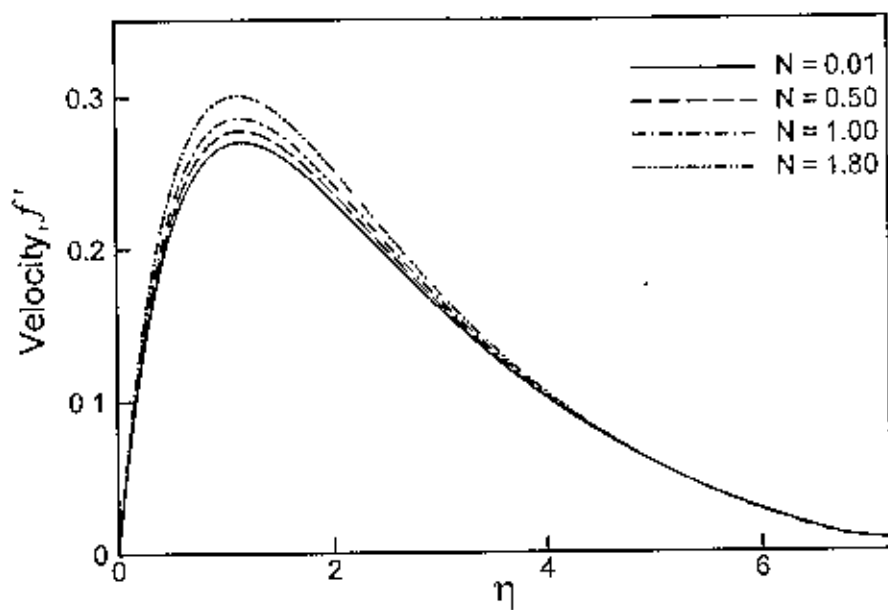


Figure 3.4: Variation of velocity profile against η for varying of N with $\gamma = 0.02$, $M = 2.6$, $J = 0.01$ and $Pr = 0.73$

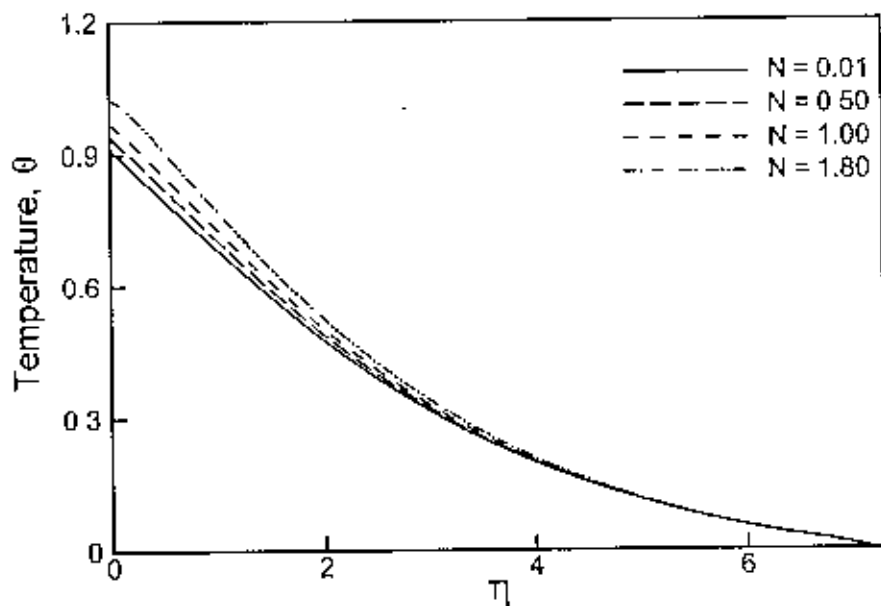


Figure 3.5: Variation of temperature profile against η for varying of N with $M = 2.6$, $\gamma = 0.02$, $J = 0.01$ and $Pr = 0.73$

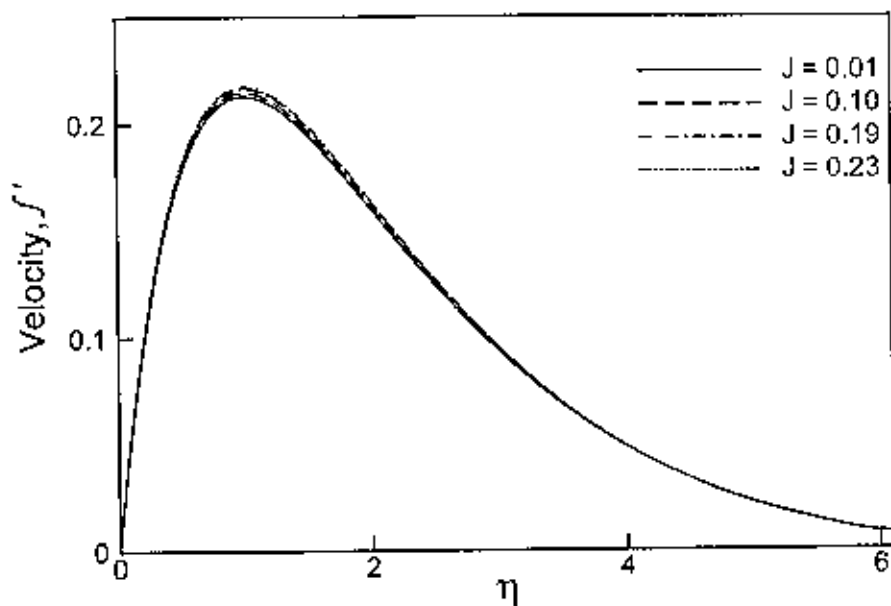


Figure 3.6: Variation of velocity profile against η for varying of J with $M = 2.6$, $\gamma = 0.01$, $N = 0.01$ and $Pr = 1.73$

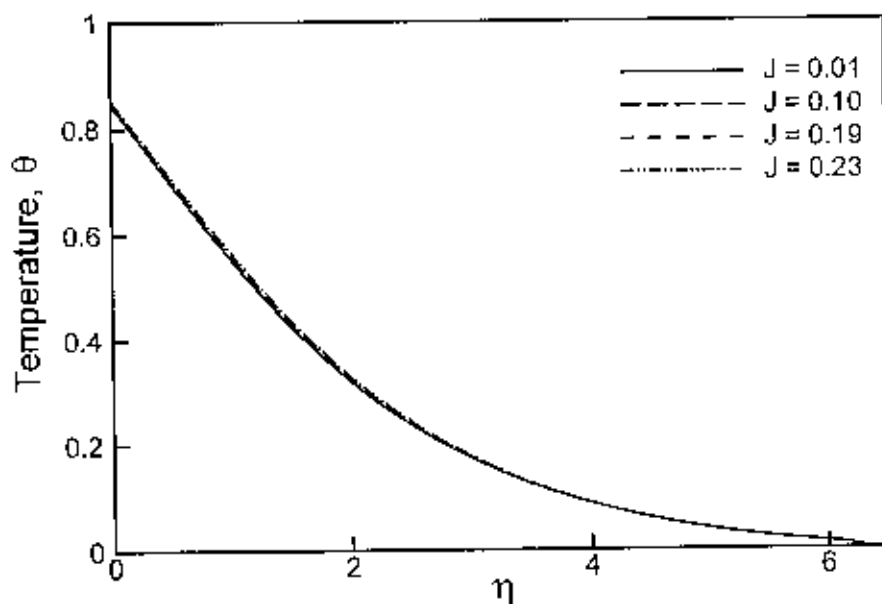


Figure 3.7: Variation of temperature profile against η for varying of J with $M = 2.6$, $\gamma = 0.01$, $N = 0.01$ and $Pr = 1.73$

Table 3.1: Skin friction coefficient and surface temperature profile against x for different values of viscous dissipation parameter N with other controlling parameters $M = 2.6$, $\gamma = 0.02$, $J = 0.01$ and $Pr = 0.73$

x	$N = 0.01$		$N = 0.50$		$N = 1.00$		$N = 1.80$	
	C_{fx}	θ	C_{fx}	θ	C_{fx}	θ	C_{fx}	θ
1.1752	0.6435	0.8060	0.6654	0.8304	0.6900	0.8584	0.7354	0.9112
2.3756	0.6958	0.8469	0.7295	0.8821	0.7698	0.9251	0.8515	1.0146
3.4792	0.7219	0.8664	0.7633	0.9086	0.8149	0.9619	0.9272	1.0818
4.5494	0.7388	0.8790	0.7861	0.9263	0.8469	0.9880	0.9879	1.1362
5.6929	0.7519	0.8888	0.8045	0.9405	0.8738	1.0100	1.0452	1.1882
6.8315	0.7619	0.8962	0.8188	0.9516	0.8957	1.0280	1.0978	1.2364
7.7112	0.7681	0.9008	0.8280	0.9588	0.9103	1.0400	1.1366	1.2723
8.8791	0.7751	0.9060	0.8385	0.9669	0.9274	1.0541	1.1868	1.3193
10.0179	0.7807	0.9103	0.8471	0.9737	0.9421	1.0662	1.2354	1.3652
12.0026	0.7887	0.9163	0.8597	0.9836	0.9642	1.0846	1.3213	1.4478
15.2684	0.7983	0.9236	0.8756	0.9962	0.9941	1.1098	1.4764	1.6009

Figure 3.8 and figure 3.9 deal with the effect of prandtl number on the skin friction coefficient and surface temperature profile against x with $M = 0.02$, $N = 0.02$, $J = 0.01$ and $\gamma = 0.1$. It can be observed from figure 3.8 that the skin friction coefficient increases monotonically for a particular value of Pr . It can also be noted that the skin friction coefficients decrease for the increasing Pr . From figure 3.9. It can be seen that the surface temperature profile decreases for the increasing Pr .

The effect of viscous dissipation parameter on the skin friction coefficient and surface temperature profile against x with $M = 2.6$, $\gamma = 0.02$, $J = 0.01$ and $Pr = 0.73$ are shown in figure 3.10 and figure 3.11, respectively. It is observed from figure 3.10 that the skin friction coefficient increases monotonically for a particular value of N . From figure 3.11 it can be seen that the surface temperature profile increases for increasing N from 0.01 to 1.80.

The variation of skin friction coefficient and surface temperature profile for different values of J with $\gamma = 0.01$, $N = 0.01$, $M = 2.6$ and $Pr = 1.73$ at different positions are

illustrated in figure 3.12 and figure 3.13 respectively. It is observed from figure 3.12 that the increasing values of the Joule heating parameter J leads to an increase in the skin friction factor. Again figure 3.13 shows that the surface temperature increases due to the increasing values of J .

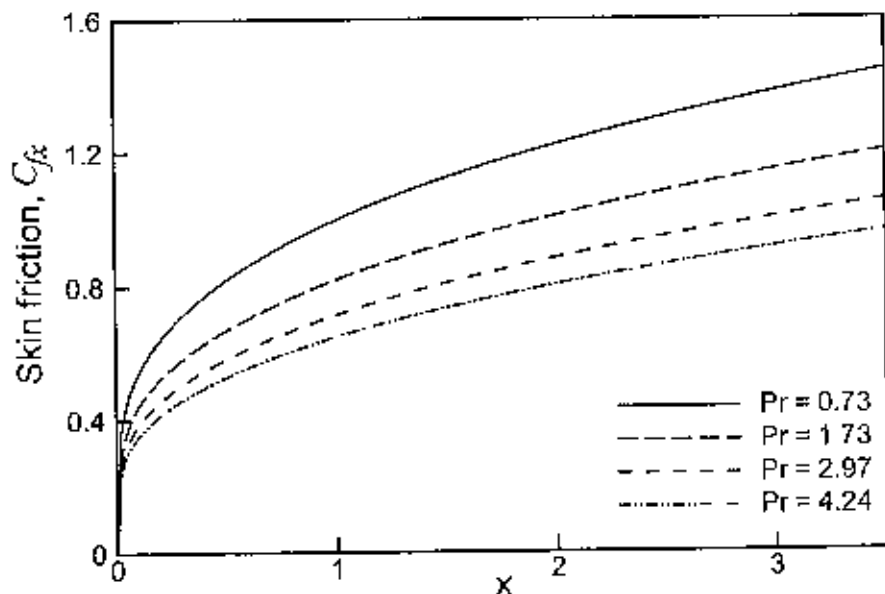


Figure 3.8: Variation of skin friction coefficient against x for varying of Pr with $M = 0.02$, $N = 0.02$, $J = 0.01$ and $\gamma = 0.1$

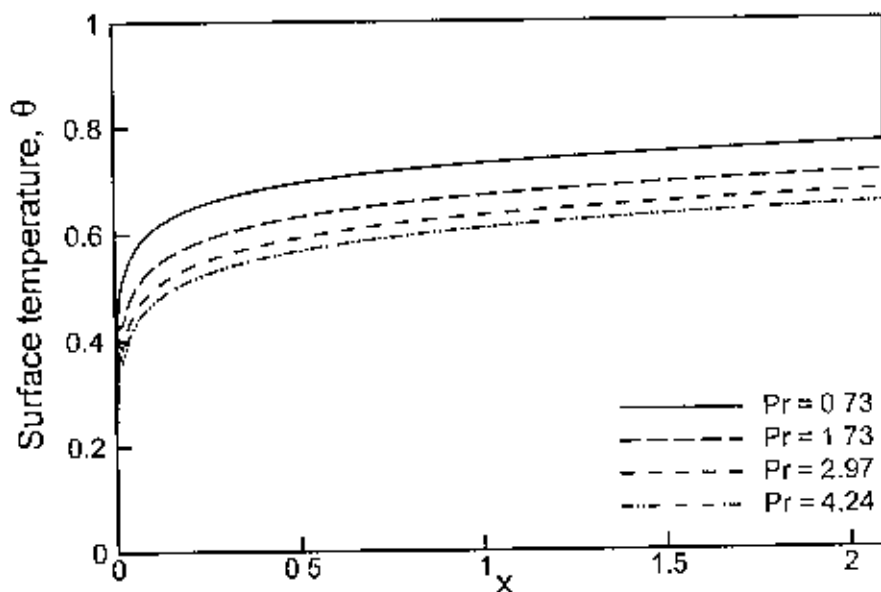


Figure 3.9: Variation of surface temperature profile against x for varying of Pr with $M = 0.02$, $N = 0.02$, $J = 0.01$ and $\gamma = 0.1$

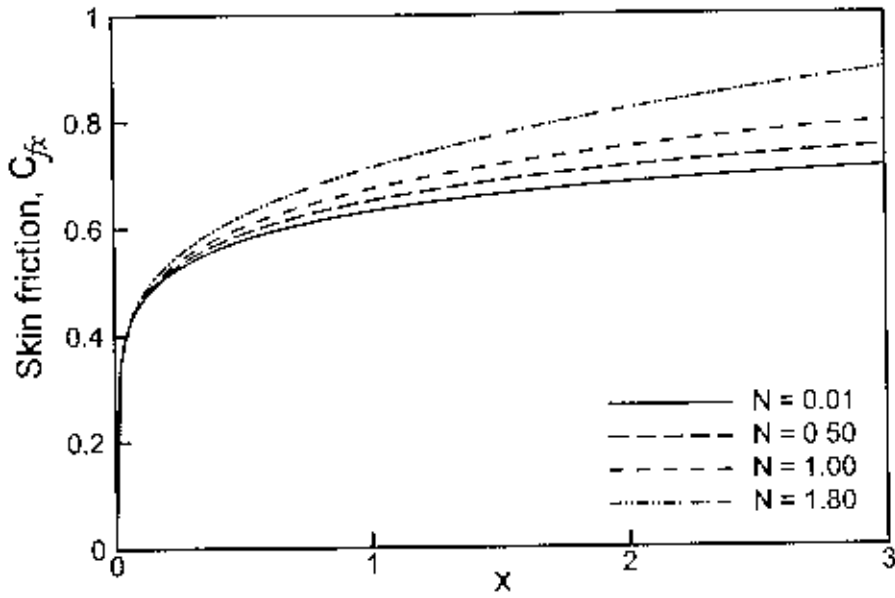


Figure 3.10: Variation of skin friction coefficient against x for varying of N with $M = 2.6$, $\gamma = 0.02$, $J = 0.01$ and $Pr = 0.73$

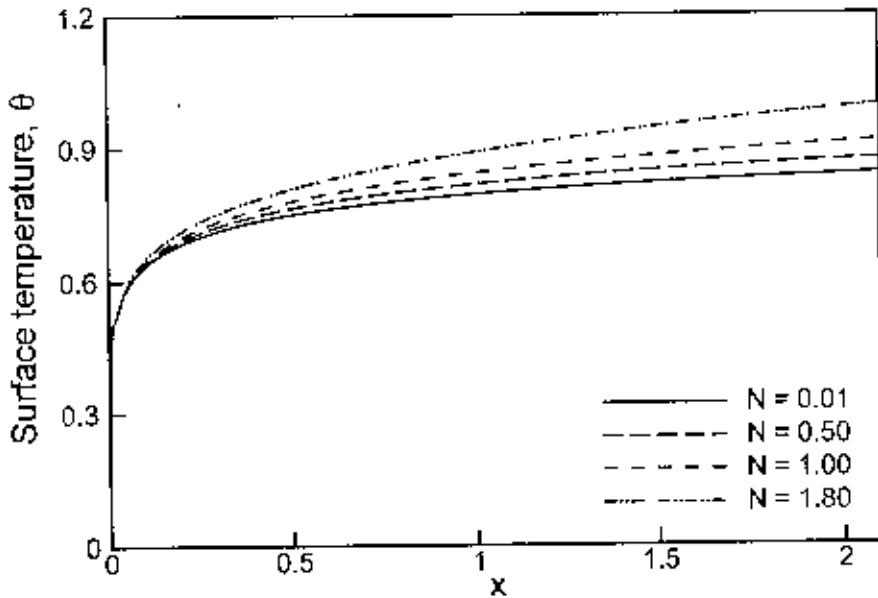


Figure 3.11: Variation of surface temperature profile against x for varying of N with $M = 2.6$, $\gamma = 0.02$, $J = 0.01$ and $Pr = 0.73$

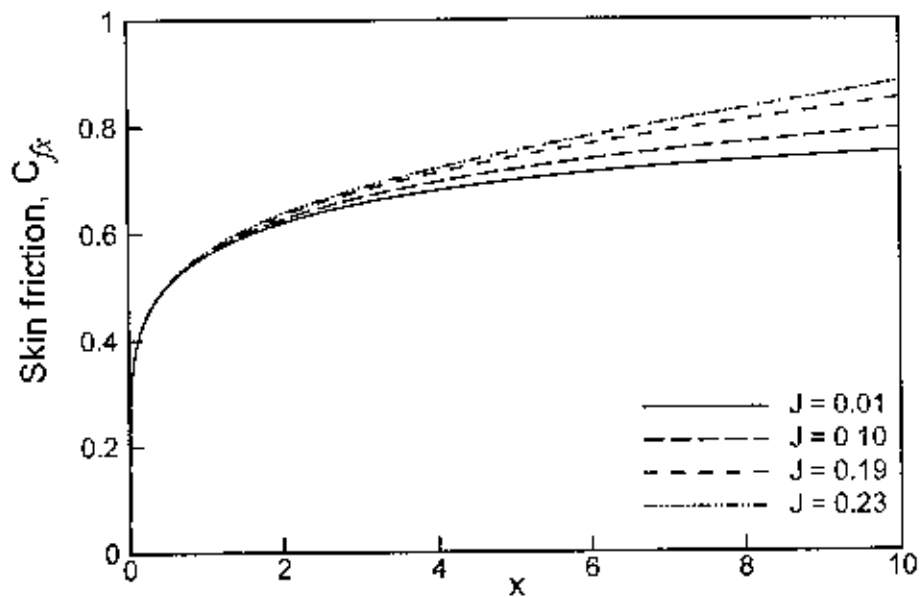


Figure 3.12: Variation of skin friction coefficient against x for varying of J with $M = 2.6$, $\gamma = 0.01$, $N = 0.01$ and $Pr = 1.73$

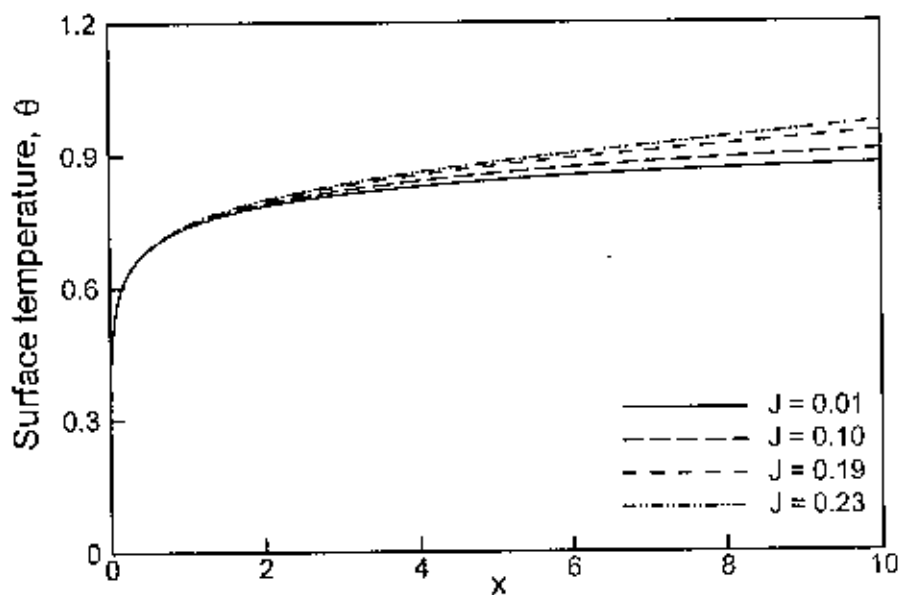


Figure 3.13: Variation of surface temperature profile against x for varying of J with $M = 2.6$, $\gamma = 0.01$, $N = 0.01$ and $Pr = 1.73$

3.5 Comparison of effect of N

The comparison of the effects of thermal conductivity variation parameter γ on the velocity profile within the boundary layer with other controlling parameters $M = 0.01$, $J = 0.01$ and $Pr = 0.73$ (having the effect of $N = 0.0$ and $N = 0.1$) are shown in figure 3.14 and figure 3.15, respectively. In figure 3.14, maximum values of velocity are 0.5937, 0.6138, 0.6234, and 0.6416 due to values of $\gamma = 0.01, 0.21, 0.31$ and 0.51 respectively. Each of them occurs at $\eta = 0.2808$. Velocity profile increases by 7.47% when γ increases from 0.01 to 0.51. From figure 3.15 it is noted that maximum values of velocity are 0.5876, 0.6076, 0.6171 and 0.6352 in the case of using $N = 0.1$. Here velocity increases by 7.51%.

Figures 3.16 and 3.17 show the comparison on temperature profile within the boundary layer for the effects of γ using the parameter $N = 0.0$ and $N = 0.1$ respectively. Maximum values of temperature are obtained 0.8293, 0.8397, 0.8441 and 0.8516 from figure 3.16. Each of them occurs at the interface. Temperature profile increases by 2.62% in the absence of effect of viscous dissipation parameter N ($N = 0.0$). Maximum values of temperature are 0.8451, 0.8553, 0.8595 and 0.8667 due to increasing values of γ from 0.01 to 0.51. Temperature increases by 2.5% in the case of using $N = 0.1$.

Figure 3.18 and figure 3.19 illustrate the comparison of the effects of thermal conductivity variation parameter on the skin friction coefficient against x with other controlling parameter $M = 0.01$, $J = 0.01$ and $Pr = 0.73$. It is seen that the effect of viscous dissipation parameter is ignored ($N = 0.0$) in figure 3.18 and is used significantly ($N = 0.1$) in figure 3.19, respectively.

The comparison of the effects of γ (without and with the effect of viscous dissipation parameter N) on Surface temperature profile are shown in figure 3.20 and 3.21, respectively. It is observed that the surface temperature profile increases for both cases due to the increasing values of γ from 0.01 to 0.51. This parameter also accelerates the fluid flow and increases the surface temperature.

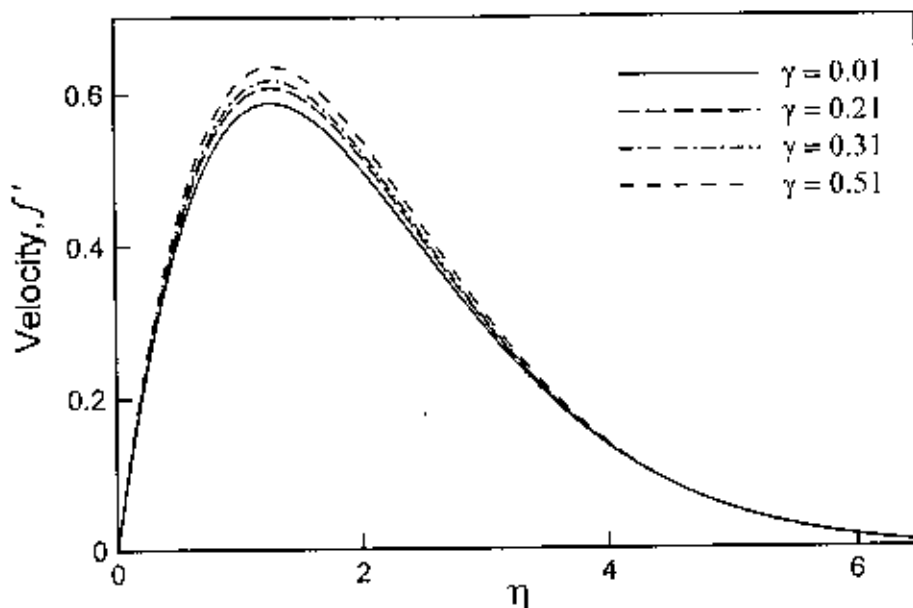


Figure 3.14: Variation of velocity profile against η for varying of γ with $M = 0.01, J = 0.01, Pr = 1.73$ and $N = 0.0$.

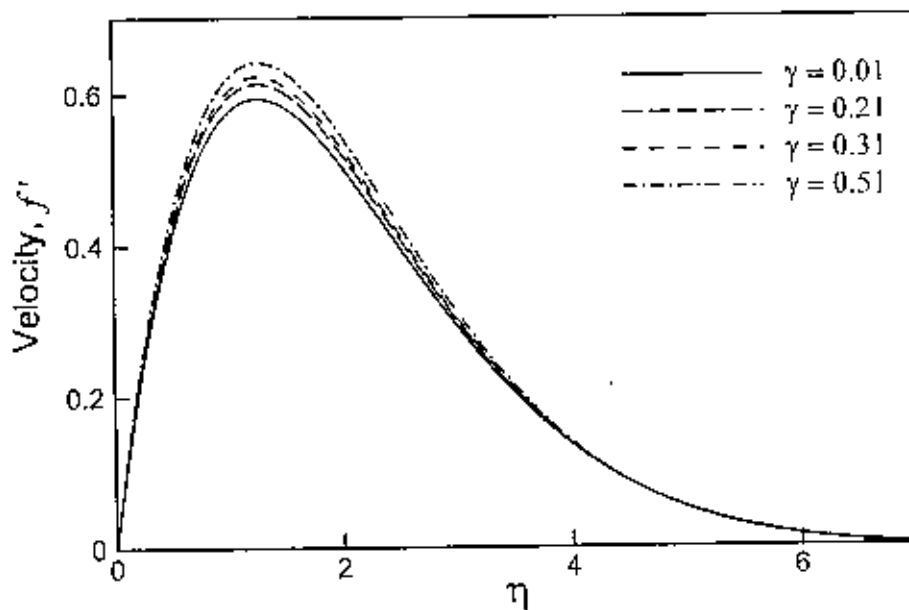


Figure 3.15: Variation of velocity profile against η for varying of γ with $M = 0.01, J = 0.01, Pr = 1.73$ and $N = 0.1$.

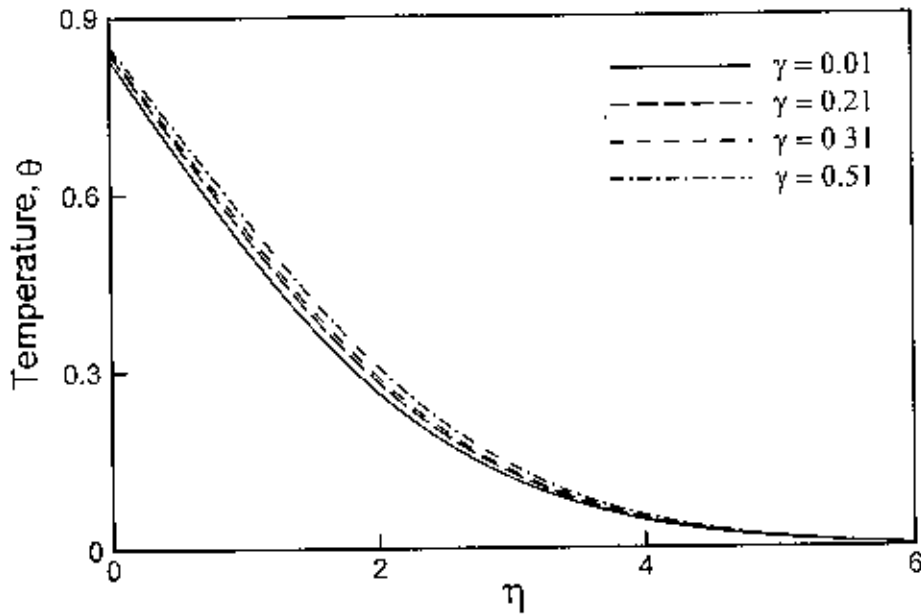


Figure 3.16: Variation of temperature profile against η for varying of γ with $M = 0.01$, $J = 0.01$, $Pr = 1.73$ and $N = 0.0$.

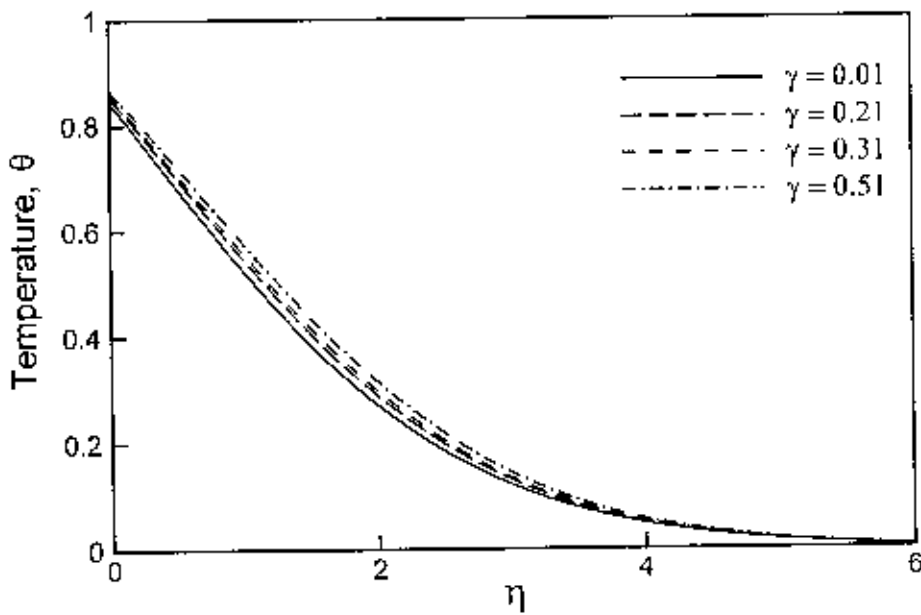


Figure 3.17: Variation of temperature profile against η for varying of γ with $M = 0.01$, $J = 0.01$, $Pr = 1.73$ and $N = 0.1$.

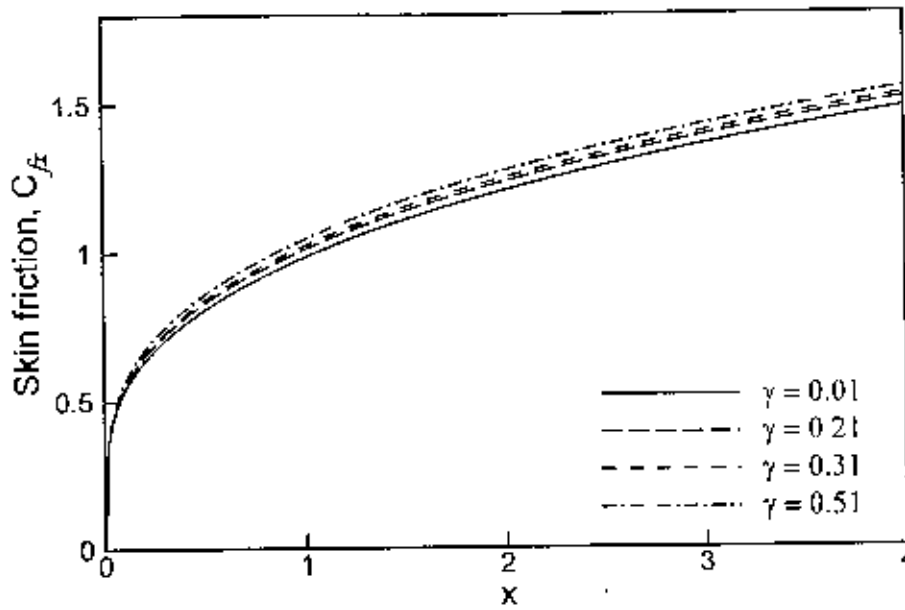


Figure 3.18: Variation of skin friction coefficient against x for varying of γ with $M = 0.01$, $J = 0.01$, $Pr = 0.73$ and $N = 0.0$.

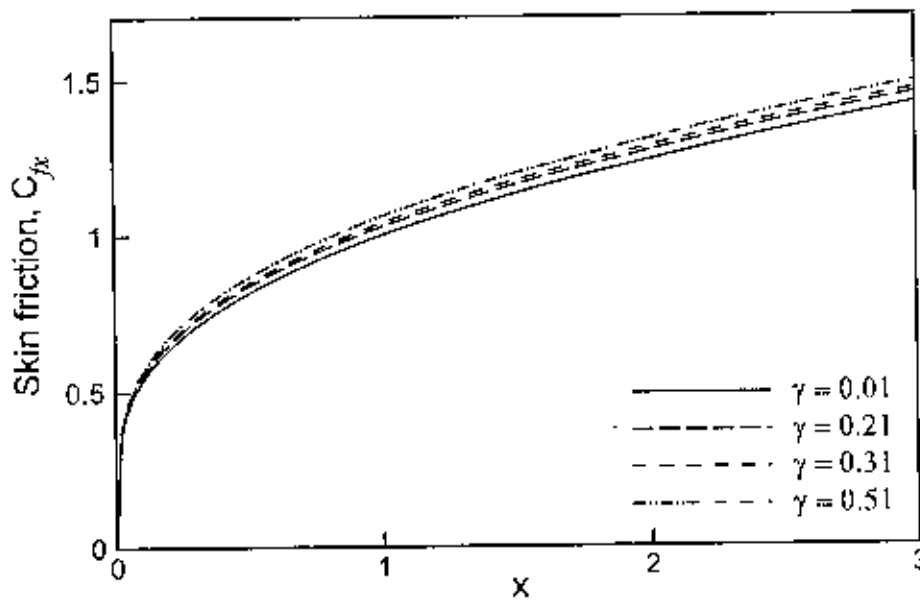


Figure 3.19: Variation of skin friction coefficient against x for varying of γ with $M = 0.01$, $J = 0.01$, $Pr = 0.73$ and $N = 0.1$.

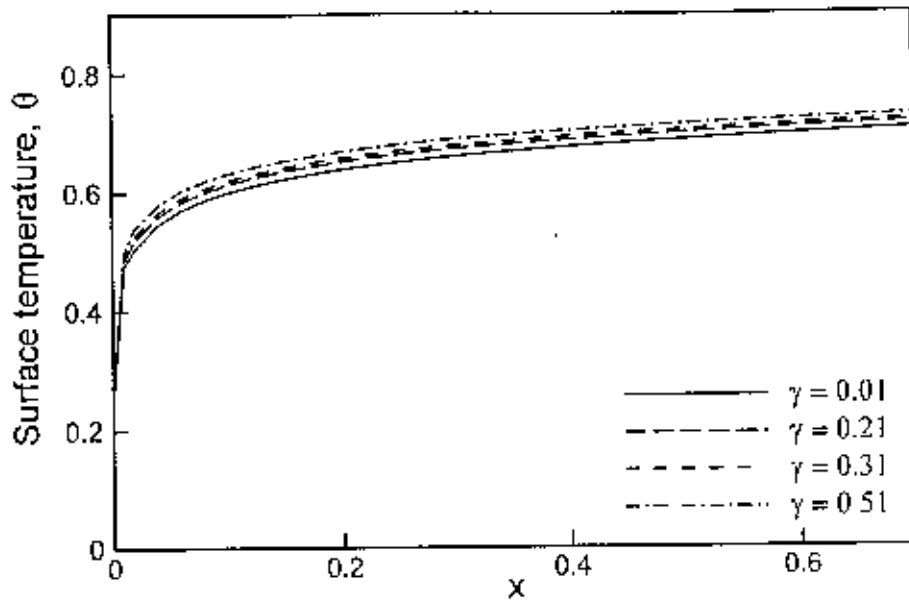


Figure 3.20: Variation of surface temperature profile against x for varying of γ with $M = 0.01$, $J = 0.01$, $Pr = 0.73$ and $N = 0.0$.

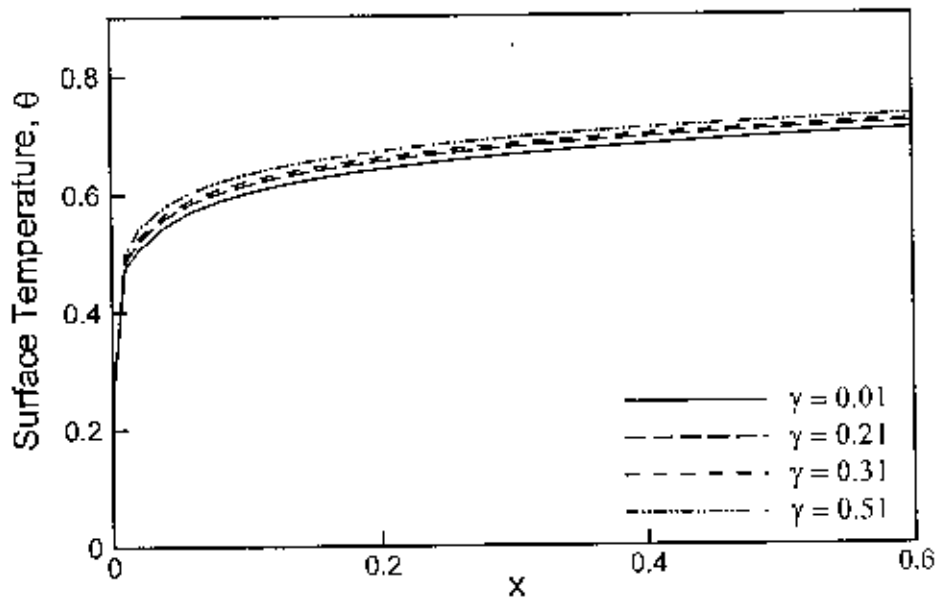


Figure 3.21: Variation of surface temperature profile against x for varying of γ with $M = 0.01$, $J = 0.01$, $Pr = 0.73$ and $N = 0.1$.

From the above figures it is observed that when there is no effect of viscous dissipation parameter N , then the figures are same as in the previous chapter. Also when the effect of

$N = 0.1$ is introduced then some variations are obtained significantly. This is because for $N = 0.1$, viscosity is dissipated and fluid velocity is increased by 7.51%, which is greater than 7.47% in the case of using $N = 0.0$. Also maximum values of temperature profile are greater for $N = 0.1$ than that of using $N = 0.0$ in each case. So additional using of viscous dissipation parameter N in this chapter signifies significant significance.

Table 3.2: Comparison of Skin friction coefficient C_f against x for different values of thermal conductivity variation parameter γ (without and with the effect of viscous dissipation parameter N) having other controlling parameters $M = 0.01$, $J = 0.01$ and $Pr = 0.73$

C_{fx}	$\gamma = 0.01$		$\gamma = 0.21$		$\gamma = 0.31$		$\gamma = 0.51$	
	$N = 0.0$	$N = 0.1$	$N = 0.0$	$N = 0.1$	$N = 0.0$	$N = 0.1$	$N = 0.0$	$N = 0.1$
0.8615	0.9434	0.9564	0.9690	0.9821	0.9807	0.9938	1.0021	1.0152
1.0847	1.0079	1.0251	1.0348	1.0521	1.0471	1.0644	1.0694	1.0867
3.1340	1.3779	1.4419	1.4080	1.4724	1.4213	1.4858	1.4452	1.5099
5.6929	1.6530	1.7903	1.6812	1.8200	1.6935	1.8329	1.7152	1.8558
7.4063	1.7967	1.9910	1.8227	2.0201	1.8339	2.0327	1.8536	2.0548
8.7021	1.8939	2.1350	1.9179	2.1646	1.9284	2.1771	1.9466	2.1991
9.6231	1.9587	2.2365	1.9814	2.2657	1.9913	2.2784	2.0085	2.3004
11.3011	2.0703	2.4188	2.0906	2.4495	2.0994	2.4626	2.1149	2.4854
14.9654	2.2433	2.8230	2.3107	2.8625	2.3177	2.8787	2.3300	2.9059

In Table 3.2, the numerical values of the skin friction coefficient C_f against x for different values of γ (with and without the effect of N) in the case of fixed values $M = 0.01$, $Pr = 0.73$, $J = 0.01$ are shown. It is observed from the table that the values of the skin friction coefficient at different position of x for $\gamma = 0.01, 0.21, 0.31, 0.51$ are lower when parameter N is not used ($N = 0.0$) than that of using $N = 0.1$. Near the axial position $x = 7.4063$, the rate of increase of the local skin friction coefficient is around 3.07% as γ changes from 0.01 to 0.51 when there is no effect of N . But applying the effect of $N = 0.1$ the corresponding rate is around 3.11% as γ changes from 0.01 to 0.51.

3.6 Conclusion

Combined effects of variable thermal conductivity and Joule heating on MHD free convection flow along a vertical flat plate with conduction and viscous dissipation has been studied. The conclusion is as follows

- Significant effects of viscous dissipation parameter N on velocity and temperature profiles as well as on skin friction coefficient and surface temperature within the boundary layer have been found in this investigation.
- The increase in Pr leads to decrease in velocity, temperature, local skin friction coefficient and surface temperature profiles.
- All the velocity, temperature, skin friction coefficient and surface temperature profiles increase significantly when the values of thermal conductivity variation parameter γ increase for both cases (without and with the effect of N).
- The increase in J leads to an increase in velocity, temperature, local skin friction coefficient and surface temperature profiles.

4.1 Conclusion

The effects of variable thermal conductivity on the coupling of conduction and Joule heating with Magnetohydrodynamic (MHD) free convection flow along a vertical flat plate in presence of viscous dissipation have been studied. From the present investigation the following conclusion may be drawn

- The velocity profile within the boundary layer increases for decreasing values of the magnetic parameter M , Prandtl number Pr and increasing values of the thermal conductivity variation parameter γ , viscous dissipation parameter N and Joule heating parameter J .
- The temperature profile within the boundary layer increases for the increasing value of magnetic parameter M , thermal conductivity variation parameter γ and viscous dissipation parameter N , Joule heating parameter J , and decreasing values of the Prandtl number Pr .
- The skin friction coefficient decreases for the increasing values of the magnetic parameter M , Prandtl number Pr and decreasing values of the thermal conductivity variation parameter γ , viscous dissipation parameter N and Joule heating parameter J .
- An increase in the values of the thermal conductivity variation parameter γ , viscous dissipation parameter N , Joule heating parameter J and magnetic parameter M leads to an increase in the surface temperature profile.
- The surface temperature profile decreases for the increasing values of the Prandtl number Pr .
- The presence of a magnetic field normal to the flow in an electrically conducting fluid introduces a Lorentz force, which acts against the flow. This resistive force tends to slow down the flow and hence the fluid velocity decreases with the increase of the magnetic parameter. There is a friction between magnetic field and fluid flow. It produces heat. As a result the temperature profile increases with the increase of the magnetic parameter and also surface temperature profile increase with the increase of M . Since the velocity decreases for the increasing values of magnetic parameter, so skin friction reduces for increasing values of M .

Conclusion

- Thermal conductivity depends on the temperature difference between the temperature outside the plate and the temperature outside the boundary layer. If this difference increases then also thermal conductivity increases, so increasing value of thermal conductivity variation parameter indicates that heat is transferred rapidly from plate to the fluid in the boundary layer. Then temperature increases within the boundary layer and also fluid mass is transferred. Increasing velocity increases skin friction coefficient and surface temperature as well.

4.2 Extension of this work

The present work may be extended in different ways. Some of those are:

- Temperature dependent thermal conductivity has been considered in the present study. For further extension temperature dependent viscosity of the fluid may be considered.
- The problem may be extended considering the Radiation heat transfer effects.
- Forced convection may be studied with the same geometry.
- It can also be considered for unsteady flow of the fluid.
- Wavy surface can also be considered here.
- This problem may be extended by considering critical behavior of the flow.

References

- Ahmad N. and Zaidi H. N., Magnetic effect on oberbeck convection through vertical stratum, Proc. 2nd BSME-ASME International Conference on Thermal Engineering, pp. 157-166, 2004.
- Al- Khawaja M. J., Agarwal R. K. and Gradner R. A., Numerical study of magneto fluid mechanics combined free and forced convection heat transfer, Int. J of Heat Mass Transfer, Vol. 42, pp. 467-475, 1999.
- Alim M. A, Alam M. and Abdullah Al-Mamun, Joule heating effect on the coupling of conduction with Magnetohydrodynamic free convection flow from a vertical flat plate. Nonlinear analysis: Modelling and Control, Vol. 12, No. 3, pp. 307-316, 2007.
- Alim M. A., Alam M., Mamun A. A. and Bellal H., Combined effect of viscous dissipation & Joule heating on the coupling of conduction & free convection along a vertical flat plate, Int. Communications of Heat & Mass Transfer, Vol 35, No. 3, pp. 338-346, 2008.
- Cebeci T. and Bradshaw P., Physical and Computational Aspects of Convective Heat Transfer, Springer, New York, 1984.
- Charraudeau J., Influence de gradients de propriétés physiques en convection force application au cas du tube, Int. J. of Heat Mass Transfer, Vol.18, pp. 87-95, 1975.
- Chen H. T and Chang S. M., The thermal interaction between laminar film condensation and forced convection along a conducting wall, Acta Mech., Vol.118, pp.13-26, 1996.
- Chen J. C., A numerical simulation of micro polar fluid flows along a flat plate with wall conduction and buoyancy effects, J. of Applied Physics D., Vol. 39, pp. 1132- 1140, 2006
- Chen P., Combined free and forced convection flow about inclined surfaces in porous media, Int. J. Heat Mass Transfer, Vol. 20, pp. 807-814, 1977.
- Chowdhury M. K. and Islam M. N., MHD free convection flow of visco-elastic fluid past an infinite porous plate, Heat Mass Transfer, Vol. 36, pp. 439-447, 2000.
- Clarke J. F. and Riley N., Natural convection induced in a gas by the presence of a hot porous horizontal surface, Q. J. Mech. Appl. Math , Vol. 28, pp 373-396, 1975
- Clarke J. F. and Riley N., Free convection and the burning of a horizontal fuel surface, J. of Fluid Mech., Vol. 74, pp. 415-431, 1976.
- El-Amin M. A., Combined effect of viscous dissipation and Joule heating on MHD forced convection over a non isothermal horizontal cylinder embedded in a fluid saturated porous medium, Journal of Magnetism and Magnetic Materials, 263(3), pp. 337-343, 2003
- Elbashbeshy E. M. A., Free convection flow with variable viscosity and thermal diffusivity along a vertical plate in the presence of magnetic field, Int. J. of Engineering Science, Vol. 38, pp. 207-213, 2000.

- Grander R. A. and Lo Y. T., Combined free and forced convection heat transfer in magneto fluid mechanic pipe flow, *AICHE*, Vol. 73, No. 164, pp.133, 1975.
- Hassanien J. A., Combined forced and free convection in boundary layer flow of a micro polar fluid over a horizontal plate, *ZAMP*, Vol. 48, No.4, pp. 571, 1977.
- Hossain M. A., The viscous and Joule heating effects on MHD free convection flow with variable plate temperature, *Int. J. of Heat Mass Transfer*, Vol. 35, No. 12, pp.3485-3487, 1992.
- Hossain M. A., Alim M. A and Rees D. A. S., The effect of radiation on free convection from a porous vertical plate, *Int. J. of Heat Mass Transfer*, Vol. 42, pp. 181-191, 1999.
- Hossain M. A., Das S. K. and Pop I., Heat transfer response of MHD free convection flow along a vertical plate to surface temperature oscillation, *Int. J. of Non-Linear Mechanics*, Vol. 33, No. 3, pp. 541-553, 1998.
- Hossain M. A. and Ahmad M., MHD forced and free convection boundary layer flow near the leading edge, *Int. J. of Heat Mass Transfer*, Vol. 33, No. 3, pp. 571-575, 1990.
- Hossain M. A., Alam K. C. A. and Rees D. A. S., MHD forced and free convection boundary layer flow along a vertical porous plate, *Applied Mechanics and Engineering*, Vol 2, No.1, pp. 33-51, 1997.
- Keller H. B., Numerical methods in boundary layer theory, *Annual Rev Fluid Mechanics*, Vol. 10, pp. 417-433, 1978.
- Khan Z. I., Conjugate effect of conduction and convection with natural convection flow from a vertical flat plate and in an inclined square cavity, M. Phil thesis, Department of Mathematics, BUET, 2002.
- Lin H. T. and Yu W. S., Free convection on a horizontal plate with blowing and suction, *J. of Heat Trans.*, ASME, Vol. 110, pp. 793-796, 1988.
- Luikov A. K., Conjugate convective heat transfer problems, *Int. J. of Heat Mass Transfer*. Vol.16, pp. 257-265, 1974.
- Mamun M. M., Azad R. and Lineeya T. R., Natural convection flow from an isothermal sphere with temperature dependent thermal conductivity, *J. of Naval Archit and Marine Engg.*, Vol. 2, pp. 53-64, 2005.
- Mamun, A. A., Azim, N. H. Md. and Maleque, Md. A., Combined Effect of Conduction and Viscous Dissipation on MHD Free Convection Flow along a Vertical Flat Plate, *J. of Naval Archit. and Marine Engg.*, Vol. 4, pp. 87-98, 2007.
- Mendez F., Trevino C., The conjugate conduction-natural convection heat transfer along a thin vertical plate with non-uniform internal heat generation, *Int. J. of Heat and Mass Transfer*, Vol. 43, pp. 2739-2748, 2000.
- Merkin J. H and Pop I., Conjugate free convection on a vertical surface, *Int. J. of Heat Mass Transfer*, Vol. 39, pp.1527- 1534, 1996.

- Merkin J. H. and Mahmood T., The free convection boundary layer flow on a vertical plate with prescribed surface heat flux, *J. of Engg. Maths.*, Vol. 24, pp. 95-107, 1990.
- Miyamoto M., Sumikawa J., Akiyoshi T. and Nakamura T., The effect of axial heat conduction in a vertical flat plate on free convection heat transfer, *Int J of Heat Mass Transfer*, Vol. 23, No.11, pp. 1545-1553, 1980.
- ÖZİŞİK M. Necati , *Heat Transfer*, New York, International Edition, 1985.
- Pop I., Lesnic D. and Ingham D. B., The conjugate mixed convection on a vertical surface in porous medium, *Int. J. of Heat Mass Transfer*, Vol. 38, No 8, pp.1517-1525. 1995.
- Pop I., Ingham D. B., *Convective heat transfer*, Pergamon, Oxford 179, 2001.
- Pozzi A. and Lupo M., The coupling of conduction with laminar convection along a flat plate, *Int. J. of Heat Mass Transfer*, Vol. 31, No. 9, pp 1807-1814, 1988.
- Raisinghania M. D., *Fluid Dynamics*, S. Chand & Company Ltd., New Delhi, 2003.
- Rahman M. M., Mamun A. A., Azim M. A., Alim M. A., Effects of temperature dependent thermal conductivity on magnetohydrodynamic free convection flow along a vertical flat plate with heat conduction, *Nonlinear Analysis: Modelling and Control*, Vol. 13, No. 4, pp. 513-524, 2008.
- Raptis A. and Kafoussias N., Magnetohydrodynamic free convection flow and mass transfer through a porous medium bounded by an infinite vertical porous plate with constant heat flux, *Canadian Journal of Physics*, Vol. 60, No 12, pp.1725-1729, 1982.
- Shu J. J. and Pop I., The thermal interaction between free convection and forced convection along a vertical conducting wall, *Int. J. of Heat Mass Transfer*, Vol 35, pp. 33-38, 1999.
- Takhar H. S. and Soundalgekar V. M., Dissipation effects on MHD free convection flow past a semi-infinite vertical plate, *Applied Scientific Research*, Vol 36, No 3, pp. 163-171, 1980.
- Vedhanayagam M., Altenkirch R. A. and Eichhorn R., A transformation of the boundary layer equations for free convection past a vertical flat plate with arbitrary blowing and wall temperature variations, *Int. J. of Heat Mass Transfer*, Vol. 23 , pp. 1286-1288, 1980.
- Wikipedia online encyclopedia, [http://en.wikipedia.org/Joule heating](http://en.wikipedia.org/Joule%20heating), 2009.

Appendix

Implicit Finite Difference Method

To get the solutions of the transformed governing equations (2.20) and (2.21) along with the boundary condition (2.22), the implicit finite difference method together with Keller box elimination technique is employed. It is well documented and widely used by Keller (1978) and Cebeci (1984).

To apply the aforementioned method, equations (2.20) and (2.21) are first converted into the following system of first order equations with dependent variables $u(\xi, \eta)$, $v(\xi, \eta)$, $p(\xi, \eta)$ and $g(\xi, \eta)$ as

$$f' = u, u' = v, g' = p \tag{A1}$$

$$v' + P_1 f v - P_2 u^2 - P_4 u + g = \xi \left(u \frac{\partial u}{\partial \xi} - v \frac{\partial f}{\partial \xi} \right) \tag{A2}$$

$$\frac{1}{Pr} p' + P_1 f p - P_3 u g + \frac{P_5}{Pr} g p' + \frac{P_2}{Pr} p^2 + P_6 u^2 = \xi \left(u \frac{\partial g}{\partial \xi} - p \frac{\partial f}{\partial \xi} \right) \tag{A3}$$

where $\xi = x$, $h = g$ and

$$P_1 = \frac{16+15x}{20(1+x)}, P_2 = \frac{6+5x}{10(1+x)}, P_3 = \frac{1}{5(1+x)}, P_4 = M x^{\frac{2}{5}} (1+x)^{\frac{1}{10}}, P_5 = \left(\frac{x}{1+x} \right)^{\frac{1}{5}} \gamma, \\ P_6 = J x^{\frac{7}{5}} (1+x)^{\frac{1}{10}}$$

and the boundary conditions are

$$f(\xi, 0) = 0, u(\xi, 0) = 0 \\ p(\xi, 0) = \frac{\xi^{\frac{1}{5}} (1+\xi)^{-\frac{1}{5}} g(\xi, 0) - 1}{(1+\xi)^{-\frac{1}{4}} + \gamma \xi^{\frac{1}{5}} (1+\xi)^{-\frac{9}{20}} g(\xi, 0)} \tag{A4}$$

$$u(\xi, 0) = 0, g(\xi, 0) = 0$$

Now consider the net rectangle on the (ξ, η) plane shown in the Figure: A-1 and denote the net points by

$$\xi^0 = 0, \xi^n = \xi^{n-1} + k_n, n = 1, 2, \dots, N \\ \eta_0 = 0, \eta_j = \eta_{j-1} + h_j, j = 1, 2, \dots, J$$

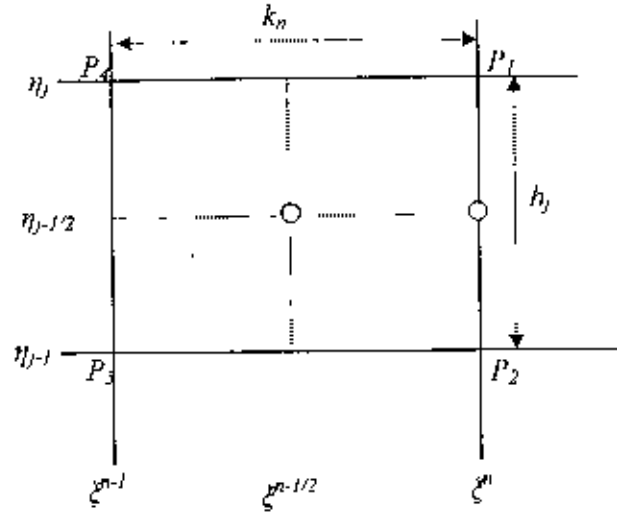


Figure: A-1 Net rectangle of difference approximations for the Box scheme.

Here n and j are just sequence of numbers on the (ξ, η) plane, k_n and h_j are the variable mesh widths. Approximate the quantities f, u, v, p at the points (ξ^n, η_j) of the net by $f_j^n, u_j^n, v_j^n, p_j^n$ which call net function. It is also employed that the notation P_j^n for the quantities midway between net points shown in Figure: A-1 and for any net function as

$$\xi^{n-1/2} = \frac{1}{2}(\xi^n + \xi^{n-1}) \quad (\text{A5})$$

$$\eta_{j-1/2} = \frac{1}{2}(\eta_j + \eta_{j-1}) \quad (\text{A6})$$

$$g_j^{n-1/2} = \frac{1}{2}(g_j^n + g_j^{n-1}) \quad (\text{A7})$$

$$g_{j-1/2}^n = \frac{1}{2}(g_j^n + g_{j-1}^n) \quad (\text{A8})$$

The finite difference approximations according to box method to the three first order ordinary differential equations (A1) are written for the mid point $(\xi^n, \eta_{j-1/2})$ of the segment P_1P_2 shown in the Figure: A-1 and the finite difference approximations to the two first order differential equations (A2) and (A3) are written for the mid point $(\xi^{n-1/2}, \eta_{j-1/2})$ of the rectangle $P_1P_2P_3P_4$. This procedure yields,

$$\frac{f_j^n - f_{j-1}^n}{h_j} = u_{j-1/2}^n = \frac{u_{j-1}^n + u_j^n}{2} \quad (\text{A9})$$

Appendix

$$\frac{u_j^n - u_{j-1}^n}{h_j} = v_{j-1/2}^n = \frac{v_{j-1}^n + v_j^n}{2} \quad (\text{A10})$$

$$\frac{g_j^n - g_{j-1}^n}{h_j} = p_{j-1/2}^n = \frac{p_{j-1}^n + p_j^n}{2} \quad (\text{A11})$$

$$\begin{aligned} & \frac{1}{2} \left(\frac{v_j^n - v_{j-1}^n}{h_j} + \frac{v_{j-1}^{n-1} - v_{j-2}^{n-1}}{h_j} \right) + P_1 (fv)_{j-1/2}^{n-1/2} - P_2 (u^2)_{j-1/2}^{n-1/2} - P_4 (u)_{j-1/2}^{n-1/2} \\ & + g_{j-1/2}^{n-1/2} = \xi_{j-1/2}^{n-1/2} \left(u_{j-1/2}^{n-1/2} \frac{u_{j-1/2}^n - u_{j-1/2}^{n-1}}{k_n} - v_{j-1/2}^{n-1/2} \frac{f_{j-1/2}^n - f_{j-1/2}^{n-1}}{k_n} \right) \end{aligned} \quad (\text{A12})$$

$$\begin{aligned} & \frac{1}{2 \text{Pr}} \left(\frac{p_j^n - p_{j-1}^n}{h_j} + \frac{p_{j-1}^{n-1} - p_{j-2}^{n-1}}{h_j} \right) + P_1 (fp)_{j-1/2}^{n-1/2} - P_3 (tg)_{j-1/2}^{n-1/2} + \\ & + \frac{P_5}{2 \text{Pr}} g_{j-1/2}^{n-1/2} \left(\frac{p_j^n - p_{j-1}^n}{h_j} + \frac{p_{j-1}^{n-1} - p_{j-2}^{n-1}}{h_j} \right) + \frac{P_5}{\text{Pr}} (p^2)_{j-1/2}^{n-1/2} + P_6 (u^2)_{j-1/2}^{n-1/2} \\ & = \xi_{j-1/2}^{n-1/2} \left(u_{j-1/2}^{n-1/2} \frac{g_{j-1/2}^n - g_{j-1/2}^{n-1}}{k_n} - p_{j-1/2}^{n-1/2} \frac{f_{j-1/2}^n - f_{j-1/2}^{n-1}}{k_n} \right) \end{aligned} \quad (\text{A13})$$

Now from the equation (A12) we have

$$\begin{aligned} & \Rightarrow \frac{1}{2} \left(\frac{v_j^n - v_{j-1}^n}{h_j} \right) + \frac{1}{2} \left(\frac{v_{j-1}^{n-1} - v_{j-2}^{n-1}}{h_j} \right) + \frac{1}{2} P_1 \{ (fv)_{j-1/2}^n + (fv)_{j-1/2}^{n-1} \} \\ & - \frac{1}{2} P_2 \{ (u^2)_{j-1/2}^n + (u^2)_{j-1/2}^{n-1} \} - \frac{1}{2} P_4 \{ u_{j-1/2}^n + u_{j-1/2}^{n-1} \} \\ & + \frac{1}{2} \{ g_{j-1/2}^n + g_{j-1/2}^{n-1} \} = \frac{1}{2k_n} \xi_{j-1/2}^{n-1/2} (u_{j-1/2}^n + u_{j-1/2}^{n-1}) (u_{j-1/2}^n - u_{j-1/2}^{n-1}) \\ & - \frac{1}{2k_n} \xi_{j-1/2}^{n-1/2} (v_{j-1/2}^n + v_{j-1/2}^{n-1}) (f_{j-1/2}^n - f_{j-1/2}^{n-1}) \end{aligned}$$

$$\begin{aligned} & \Rightarrow h_j^{-1} (v_j^n - v_{j-1}^n) + P_1 (fv)_{j-1/2}^n - P_2 (u^2)_{j-1/2}^n - P_4 (u)_{j-1/2}^n + g_{j-1/2}^n \\ & = \alpha_n \{ (u^2)_{j-1/2}^n - (u)_{j-1/2}^n (u)_{j-1/2}^{n-1} + (u)_{j-1/2}^n (u)_{j-1/2}^{n-1} \} \\ & - \{ v_{j-1/2}^n f_{j-1/2}^n - v_{j-1/2}^n f_{j-1/2}^{n-1} + f_{j-1/2}^n v_{j-1/2}^{n-1} \} - [h_j^{-1} (v_{j-1}^{n-1} - v_{j-2}^{n-1}) + P_1 (fv)_{j-1/2}^{n-1} - \\ & P_2 (u^2)_{j-1/2}^{n-1} - P_4 (u)_{j-1/2}^{n-1} + g_{j-1/2}^{n-1}] + \alpha_n [-(u^2)_{j-1/2}^{n-1} + (fv)_{j-1/2}^{n-1}] \end{aligned}$$

Appendix

$$\begin{aligned} &\Rightarrow h_j^{-1} (v_j^n - v_{j-1}^n) + P_1 (fv)_{j-1/2}^n - P_2 (u^2)_{j-1/2}^n - P_4 (u)_{j-1/2}^n + g_{j-1/2}^n \\ &- \alpha_n \left[\left\{ (u^2)_{j-1/2}^n - (fv)_{j-1/2}^n + v_{j-1/2}^n f_{j-1/2}^{n-1} - f_{j-1/2}^n v_{j-1/2}^{n-1} \right\} \right] \\ &= \alpha_n \left[(fv)_{j-1/2}^{n-1} - (u^2)_{j-1/2}^{n-1} \right] - L_{j-1/2}^{n-1} \end{aligned}$$

$$\text{where } L_{j-1/2}^{n-1} = h_j^{-1} (v_j^{n-1} - v_{j-1}^{n-1}) + P_1 (fv)_{j-1/2}^{n-1} - P_2 (u^2)_{j-1/2}^{n-1} - P_4 (u)_{j-1/2}^{n-1} + g_{j-1/2}^{n-1}$$

$$\begin{aligned} &\Rightarrow h_j^{-1} (v_j^n - v_{j-1}^n) + \{P_1 + \alpha_n\} (fv)_{j-1/2}^n - \{P_2 + \alpha_n\} (u^2)_{j-1/2}^n \\ &- P_4 (u)_{j-1/2}^n + g_{j-1/2}^n + \alpha_n (f_{j-1/2}^n v_{j-1/2}^{n-1} - v_{j-1/2}^n f_{j-1/2}^{n-1}) \\ &= \alpha_n \left\{ (fv)_{j-1/2}^{n-1} - (u^2)_{j-1/2}^{n-1} \right\} - L_{j-1/2}^{n-1} \end{aligned}$$

$$\begin{aligned} &\Rightarrow h_j^{-1} (v_j^n - v_{j-1}^n) + \{P_1 + \alpha_n\} (fv)_{j-1/2}^n - \{P_2 + \alpha_n\} (u^2)_{j-1/2}^n \\ &- P_4 (u)_{j-1/2}^n + g_{j-1/2}^n + \alpha_n (f_{j-1/2}^n v_{j-1/2}^{n-1} - v_{j-1/2}^n f_{j-1/2}^{n-1}) \tag{A14} \\ &= R_{j-1/2}^{n-1} \end{aligned}$$

$$\text{where } \alpha_n = \frac{1}{k_n} \xi_{j-1/2}^{n-1/2} \text{ and } R_{j-1/2}^{n-1} = \alpha_n \left\{ (fv)_{j-1/2}^{n-1} - (u^2)_{j-1/2}^{n-1} \right\} - L_{j-1/2}^{n-1}$$

Again from the equation (A13) then

$$\begin{aligned} &\frac{1}{2Pr} h_i^{-1} (p_j^n - p_j^{n-1} + p_{j+1}^{n-1} - p_{j-1}^{n-1}) + \frac{P_1}{2} \left\{ (fp)_{j-1/2}^n + (fp)_{j-1/2}^{n-1} \right\} \\ &- \frac{P_3}{2} \left\{ (ug)_{j-1/2}^n + (ug)_{j-1/2}^{n-1} \right\} + \frac{P_5}{4Pr} h_j^{-1} \left[\left(g_{j-1/2}^n + g_{j-1/2}^{n-1} \right) (p_j^n - p_{j+1}^{n-1} + p_{j-1}^{n-1} - p_{j-1}^{n-1}) \right] \\ &+ \frac{P_3}{2Pr} \left\{ (p^2)_{j-1/2}^n + (p^2)_{j-1/2}^{n-1} \right\} + \frac{P_6}{2} \left\{ (u^2)_{j-1/2}^n + (u^2)_{j-1/2}^{n-1} \right\} \\ &= \frac{1}{2k_n} \xi_{j-1/2}^{n-1} \left[\left(u_{j-1/2}^n + u_{j-1/2}^{n-1} \right) \left(g_{j-1/2}^n - g_{j-1/2}^{n-1} \right) - \left(p_{j-1/2}^n + p_{j-1/2}^{n-1} \right) \left(f_{j-1/2}^n - f_{j-1/2}^{n-1} \right) \right] \end{aligned}$$

$$\begin{aligned} &\Rightarrow \frac{1}{Pr} h_j^{-1} (p_j^n - p_{j-1}^n) + (P_1 + \alpha_n) (fp)_{j-1/2}^n - (P_3 + \alpha_n) (ug)_{j-1/2}^n \\ &+ \frac{P_5}{2Pr} h_j^{-1} g_{j-1/2}^n (p_j^n - p_{j+1}^{n-1} + p_j^{n-1} - p_{j-1}^{n-1}) + \frac{P_3}{2Pr} h_j^{-1} g_{j-1/2}^{n-1} (p_j^n - p_{j-1}^n) + \frac{P_3}{Pr} (p^2)_{j-1/2}^n \\ &+ P_6 (u^2)_{j-1/2}^n + \alpha_n \left[u_{j-1/2}^n g_{j-1/2}^{n-1} - g_{j-1/2}^n u_{j-1/2}^{n-1} - p_{j-1/2}^n f_{j-1/2}^{n-1} + f_{j-1/2}^n p_{j-1/2}^{n-1} \right] \\ &= \alpha_n \left[(fp)_{j-1/2}^{n-1} - (ug)_{j-1/2}^{n-1} \right] - M_{j-1/2}^{n-1} \end{aligned}$$

where,

Appendix

$$\begin{aligned}
 M_{j-\frac{1}{2}}^{n-1} &= \frac{h_j^{-1}}{\text{Pr}} \{p_j^{n-1} - p_{j-1}^{n-1}\} + P_1 (fp)_{j-\frac{1}{2}}^{n-1} - P_3 (ug)_{j-\frac{1}{2}}^{n-1} + \frac{P_5}{\text{Pr}} (p^2)_{j-\frac{1}{2}}^{n-1} + P_6 (u^2)_{j-\frac{1}{2}}^{n-1} \\
 &+ \frac{P_5 h_j^{-1}}{2 \text{Pr}} g_{j-\frac{1}{2}}^{n-1} \{p_j^{n-1} - p_{j-1}^{n-1}\} \\
 &\Rightarrow \frac{1}{\text{Pr}} h_j^{-1} (p_j^n - p_{j-1}^n) + (P_1 + \alpha_n) (fp)_{j-1/2}^n - (P_3 + \alpha_n) (ug)_{j-1/2}^n \\
 &+ \frac{P_5}{2 \text{Pr}} h_j^{-1} g_{j-1/2}^n (p_j^n - p_{j-1}^n + p_j^{n-1} - p_{j-1}^{n-1}) + \frac{P_5}{2 \text{Pr}} h_j^{-1} g_{j-1/2}^{n-1} (p_j^n - p_{j-1}^n) \\
 &+ P_6 (u^2)_{j-\frac{1}{2}}^n + \frac{P_5}{\text{Pr}} (p^2)_{j-\frac{1}{2}}^n + \alpha_n [u_{j-1/2}^n g_{j-1/2}^{n-1} - g_{j-1/2}^n u_{j-1/2}^{n-1} - p_{j-1/2}^n f_{j-1/2}^{n-1} \\
 &+ f_{j-1/2}^n p_{j-1/2}^{n-1}] = T_{j-1/2}^{n-1}
 \end{aligned} \tag{A15}$$

where $T_{j-1/2}^{n-1} = -M_{j-1/2}^{n-1} + \alpha_n \{ (fp)_{j-1/2}^{n-1} - (ug)_{j-1/2}^{n-1} \}$

The boundary condition becomes

$$\begin{aligned}
 f_0^n &= 0, \quad u_0^n = 0, \\
 p_0^n(\xi, 0) &= \frac{\xi^{\frac{1}{3}}(1+\xi)^{\frac{1}{3}} g_0^n - 1}{(1+\xi)^{\frac{1}{4}} + \gamma \xi^{1/3}(1+\xi)^{\frac{2}{3}} g_0^n}
 \end{aligned} \tag{A16}$$

$$u_j^n = 0, \quad g_j^n = 0$$

It is assumed that $f_j^{n-1}, u_j^{n-1}, v_j^{n-1}, g_j^{n-1}, p_j^{n-1}$, for $0 \leq j \leq J$ are known. Then equations (A5) to (A15) form a system of $5J+5$ non linear equations for the solutions of the $5J+5$ unknowns $(f_j^n, u_j^n, v_j^n, g_j^n, p_j^n)$, $j = 0, 1, 2, 3, \dots, J$. These non-linear systems of algebraic equations are to be linearized by Newton's Quassy linearization method. The iterates $(f_j^i, u_j^i, v_j^i, g_j^i, p_j^i)$, $i = 0, 1, 2, 3, \dots, N$, are defined with initial values equal those at the previous x-station for the higher iterates. Thus the following forms can be written

$$f_j^{(i+1)} = f_j^i + \delta f_j^i \tag{A17}$$

$$u_j^{(i+1)} = u_j^i + \delta u_j^i \tag{A18}$$

$$v_j^{(i+1)} = v_j^i + \delta v_j^i \tag{A19}$$

$$g_j^{(i+1)} = g_j^i + \delta g_j^i \tag{A20}$$

$$p_j^{(i+1)} = p_j^i + \delta p_j^i \tag{A21}$$

Now by substituting the right hand sides of the above equations in place of $f_j^{(n)}, u_j^{(n)}, v_j^{(n)}$ and $g_j^{(n)}$ dropping the terms that are quadratic in $\delta f_j^{(n)}, \delta u_j^{(n)}, \delta v_j^{(n)}$ and $\delta p_j^{(n)}$, the equations (A9), (A10) and (A11) then take the following linear system of algebraic form

$$f_j^{(n)} + \delta f_j^{(n)} - f_{j-1}^{(n)} - \delta f_{j-1}^{(n)} = \frac{h_j}{2} \{u_j^{(n)} + \delta u_j^{(n)} + u_{j+1}^{(n)} + \delta u_{j+1}^{(n)}\}$$

$$\delta f_j^{(n)} - \delta f_{j-1}^{(n)} - \frac{h_j}{2} (\delta u_j^{(n)} + \delta u_{j-1}^{(n)}) = (r_1)_j, \quad (\text{A22})$$

$$\delta u_j^{(n)} - \delta u_{j-1}^{(n)} - \frac{h_j}{2} (\delta v_j^{(n)} + \delta v_{j-1}^{(n)}) = (r_4)_j, \quad (\text{A23})$$

$$\delta g_j^{(n)} - \delta g_{j-1}^{(n)} - \frac{h_j}{2} (\delta p_j^{(n)} + \delta p_{j-1}^{(n)}) = (r_5)_j, \quad (\text{A24})$$

where, $(r_1)_j = f_{j-1}^{(n)} - f_j^{(n)} + h_j u_{j-1/2}^{(n)}$

$$(r_4)_j = u_{j-1}^{(n)} - u_j^{(n)} + h_j v_{j-1/2}^{(n)}$$

$$(r_5)_j = g_{j-1}^{(n)} - g_j^{(n)} + h_j p_{j-1/2}^{(n)}$$

Then equation (A14) becomes,

$$\begin{aligned} & h_j^{-1} \{v_j^{(n)} + \delta v_j^{(n)} - v_{j-1}^{(n)} - \delta v_{j-1}^{(n)}\} + \left(\frac{P_1 + \alpha_n}{2} \right) \{ (fv)_j^{(n)} + \delta (fv)_j^{(n)} + (fv)_{j-1}^{(n)} + \delta (fv)_{j-1}^{(n)} \} \\ & - \left(\frac{P_2 + \alpha_n}{2} \right) \{ (u^2)_j^{(n)} + \delta (u^2)_j^{(n)} + (u^2)_{j-1}^{(n)} + \delta (u^2)_{j-1}^{(n)} \} - \frac{P_3}{2} \{ (u)_j^{(n)} + \delta (u)_j^{(n)} + (u)_{j-1}^{(n)} + \delta (u)_{j-1}^{(n)} \} \\ & + \frac{1}{2} \{ g_j^{(n)} + \delta g_j^{(n)} + g_{j-1}^{(n)} + \delta g_{j-1}^{(n)} \} + \frac{\alpha_n}{2} \{ f_j^{(n)} + \delta f_j^{(n)} + f_{j-1}^{(n)} + \delta f_{j-1}^{(n)} \} v_{j-1/2}^{n-1} \\ & - \frac{\alpha_n}{2} \{ v_j^{(n)} + \delta v_j^{(n)} + v_{j-1}^{(n)} + \delta v_{j-1}^{(n)} \} f_{j-1/2}^{n-1} = R_{j-1/2}^{n-1} \end{aligned}$$

$$\begin{aligned} \Rightarrow & \delta v_j^{(n)} \left[h_j^{-1} + \frac{P_1 + \alpha_n}{2} f_j^{(n)} - \frac{\alpha_n}{2} f_{j-1/2}^{n-1} \right] + \delta v_{j-1}^{(n)} \left[-h_j^{-1} + \frac{P_1 + \alpha_n}{2} f_j^{(n)} - \frac{\alpha_n}{2} f_{j-1/2}^{n-1} \right] \\ & + \delta f_j^{(n)} \left[\frac{P_1 + \alpha_n}{2} v_j^{(n)} + \frac{\alpha_n}{2} v_{j-1/2}^{n-1} \right] + \delta f_{j-1}^{(n)} \left[\frac{P_1 + \alpha_n}{2} v_{j-1}^{(n)} + \frac{\alpha_n}{2} v_{j-1/2}^{n-1} \right] \\ & + \delta u_j^{(n)} \left[-(P_2 + \alpha_n) u_j^{(n)} - \frac{P_4}{2} \right] + \delta u_{j-1}^{(n)} \left[-(P_2 + \alpha_n) u_{j-1}^{(n)} - \frac{P_4}{2} \right] \\ & + \delta g_j^{(n)} [1/2] + \delta g_{j-1}^{(n)} [1/2] = (r_2)_j \end{aligned}$$

Appendix

$$\begin{aligned} \Rightarrow (s_1)_j \delta v_j^{(i)} + (s_2)_j \delta v_{j-1}^{(i)} + (s_3)_j \delta f_j^{(i)} + (s_4)_j \delta f_{j-1}^{(i)} + (s_5)_j \delta u_j^{(i)} \\ + (s_6)_j \delta u_{j-1}^{(i)} + (s_7)_j \delta g_j^{(i)} + (s_8)_j \delta g_{j-1}^{(i)} + (s_9)_j \cdot 0 + (s_{10})_j \cdot 0 = (r_2)_j \end{aligned} \quad (A25)$$

$$\text{where, } (s_1)_j = h_j^{-1} + \frac{P_1 + \alpha_n}{2} f_j^{(i)} - \frac{\alpha_n}{2} f_{j-1/2}^{n-1}$$

$$(s_2)_j = -h_j^{-1} + \frac{P_1 + \alpha_n}{2} f_j^{(i)} - \frac{\alpha_n}{2} f_{j-1/2}^{n-1}$$

$$(s_3)_j = \frac{(P_1 + \alpha_n)}{2} v_j^{(i)} + \frac{\alpha_n}{2} v_{j-1/2}^{n-1}$$

$$(s_4)_j = \frac{(P_1 + \alpha_n)}{2} v_{j-1}^{(i)} + \frac{\alpha_n}{2} v_{j-1/2}^{n-1}$$

$$(s_5)_j = -(P_2 + \alpha_n) u_j^{(i)} - \frac{P_4}{2}$$

$$(s_6)_j = -(P_2 + \alpha_n) u_{j-1}^{(i)} - \frac{P_4}{2}$$

$$(s_7)_j = [1/2]$$

$$(s_8)_j = [1/2]$$

$$(s_9)_j = 0$$

$$(s_{10})_j = 0$$

$$\begin{aligned} (r_2)_j = R_{j-1/2}^{n-1} - h_j^{-1} (v_j^{(i)} - v_{j-1}^{(i)}) - \frac{(P_1 + \alpha_n)}{2} \{ (fv)_j^{(i)} + (fv)_{j-1}^{(i)} \} \\ + \frac{(P_2 + \alpha_n)}{2} \{ (u^2)_j^{(i)} + (u^2)_{j-1}^{(i)} \} + \frac{P_4}{2} (u_j^{(i)} + u_{j-1}^{(i)}) - \frac{1}{2} (g_j^{(i)} + g_{j-1}^{(i)}) \\ - \frac{\alpha_n}{2} (f_j^{(i)} + f_{j-1}^{(i)}) v_{j-1/2}^{n-1} + \frac{\alpha_n}{2} (v_j^{(i)} + v_{j-1}^{(i)}) f_{j-1/2}^{n-1} \end{aligned} \quad (A26)$$

Here the coefficients $(s_9)_j$ and $(s_{10})_j$, which are zero in this case, are included here for the generality. Similarly by using the equations (A17) to (A21), then the equation (A15) can be written as

$$\begin{aligned}
&\Rightarrow \frac{1}{Pr} h_j^{-1} \{p_j' + \delta p_j' - p_{j-1}' - \delta p_{j-1}'\} + \frac{(P_1 + \alpha_n)}{2} \{(fp)'_j + \delta(fp)'_j + (fp)'_{j-1} + \delta(fp)'_{j-1}\} \\
&- \frac{(P_3 + \alpha_n)}{2} \{(ug)'_j + \delta(ug)'_j + (ug)'_{j-1} + \delta(ug)'_{j-1}\} + \frac{P_5 h_j^{-1}}{4Pr} \{g_j' + \delta g_{j-1}' + g_j' + \delta g_{j-1}'\} \\
&\{p_j^n - p_{j-1}^n + p_j^{n-1} - p_{j-1}^{n-1}\} + \frac{P_5 h_j^{-1}}{2Pr} g_{j-\frac{1}{2}}^{n-1} \{p_j' + \delta p_j' - p_{j-1}' - \delta p_{j-1}'\} + \frac{P_5}{2Pr} \{(p^2)'_j + \\
&\delta(p^2)'_j + (p^2)'_{j-1} + \delta(p^2)'_{j-1}\} + \frac{P_6}{2} \{(u^2)'_j + \delta(u^2)'_j + (u^2)'_{j-1} + \delta(u^2)'_{j-1}\} \\
&+ \frac{\alpha_n}{2} [\{u_j' + \delta u_j' + u_{j-1}' + \delta u_{j-1}'\} g_{j-\frac{1}{2}}^{n-1} - \{g_j' + \delta g_j' + g_{j-1}' + \delta g_{j-1}'\} u_{j-\frac{1}{2}}^{n-1} - (p_j' + \delta p_j' + p_{j-1}' \\
&+ \delta p_{j-1}') f_{j-\frac{1}{2}}^{n-1} + (f_j' + \delta f_j' + f_{j-1}' + \delta f_{j-1}') p_{j-\frac{1}{2}}^{n-1}] = \gamma_{j-\frac{1}{2}}^{n-1}
\end{aligned}$$

$$\begin{aligned}
&\Rightarrow \delta p_j'' \left[\frac{h_j^{-1}}{Pr} + \frac{P_1 P}{2} f_j' + \frac{P_5 h_j^{-1}}{2Pr} g_{j-\frac{1}{2}}^{n-1} + \frac{P_5}{Pr} p_j' - \frac{\alpha_n}{2} f_{j-\frac{1}{2}}^{n-1} \right] \\
&+ \delta p_{j-1}'' \left[-\frac{h_j^{-1}}{Pr} + \frac{P_1 P}{2} f_j' - \frac{P_5 h_j^{-1}}{2Pr} g_{j-\frac{1}{2}}^{n-1} + \frac{P_5}{Pr} p_j' - \frac{\alpha_n}{2} f_{j-\frac{1}{2}}^{n-1} \right] \\
&+ \delta f_j'' \left[\frac{P_1 P}{2} p_j' + \frac{\alpha_n}{2} p_{j-\frac{1}{2}}^{n-1} \right] + \delta f_{j-1}'' \left[\frac{P_1 P}{2} p_j' + \frac{\alpha_n}{2} p_{j-\frac{1}{2}}^{n-1} \right] \\
&+ \delta u_j'' \left[\frac{P_3 P}{2} g_j' + \frac{\alpha_n}{2} g_{j-\frac{1}{2}}^{n-1} + P_6 u_j' \right] + \delta u_{j-1}'' \left[-\frac{P_3 P}{2} g_j' + \frac{\alpha_n}{2} g_{j-\frac{1}{2}}^{n-1} + P_6 u_{j-1}' \right] \\
&+ \delta g_j'' \left[-\frac{P_3 P}{2} u_j' + \frac{P_5}{4Pr} \{p_j^n - p_{j-1}^n + p_j^{n-1} - p_{j-1}^{n-1}\} - \frac{\alpha_n}{2} u_{j-\frac{1}{2}}^{n-1} \right] \\
&+ \delta g_{j-1}'' \left[-\frac{P_3 P}{2} u_j' + \frac{P_5}{4Pr} \{p_j^n - p_{j-1}^n + p_j^{n-1} - p_{j-1}^{n-1}\} - \frac{\alpha_n}{2} u_{j-\frac{1}{2}}^{n-1} \right] = (r_3)_j
\end{aligned}$$

$$\begin{aligned}
&(t_1)_j \delta p_j^{(0)} + (t_2)_j \delta p_{j-1}^{(0)} + (t_3)_j \delta f_j^{(0)} + (t_4)_j \delta f_{j-1}^{(0)} + (t_5)_j \delta u_j^{(0)} \\
&+ (t_6)_j \delta u_{j-1}^{(0)} + (t_7)_j \delta g_j^{(0)} + (t_8)_j \delta g_{j-1}^{(0)} + (t_9)_j \delta v_j^{(0)} + (t_{10})_j \delta v_{j-1}^{(0)} = (r_3)_j
\end{aligned} \tag{A27}$$

$$\text{where, } (t_1)_j = \frac{1}{Pr} h_j^{-1} + \frac{(P_1 + \alpha_n)}{2} f_j^{(0)} + \frac{P_5}{2Pr} h_j^{-1} g_{j-\frac{1}{2}}^{n-1} + \frac{P_5}{Pr} p_j' - \frac{\alpha_n}{2} f_{j-\frac{1}{2}}^{n-1}$$

$$(t_2)_j = -\frac{1}{Pr} h_j^{-1} + \frac{(P_1 + \alpha_n)}{2} f_{j-1}^{(0)} - \frac{P_5}{2Pr} h_j^{-1} g_{j-\frac{1}{2}}^{n-1} + \frac{P_5}{Pr} p_{j-1}' - \frac{\alpha_n}{2} f_{j-\frac{1}{2}}^{n-1}$$

$$(t_3)_j = \frac{(P_1 + \alpha_n)}{2} p_j^{(0)} + \frac{\alpha_n}{2} p_{j-\frac{1}{2}}^{n-1}$$

$$(t_4)_j = \frac{(P_1 + \alpha_n)}{2} p_{j-1}^{(0)} + \frac{\alpha_n}{2} p_{j-\frac{1}{2}}^{n-1}$$

$$(t_5)_j = -\frac{(P_3 + \alpha_n)}{2} g_j^{(i)} + P_6 u_j^i + \frac{\alpha_n}{2} g_{j-1/2}^{n-1}$$

$$(t_6)_j = -\frac{(P_3 + \alpha_n)}{2} g_{j-1}^{(i)} + P_6 u_{j-1}^i + \frac{\alpha_n}{2} g_{j-1/2}^{n-1}$$

$$(t_7)_j = -\frac{(P_3 + \alpha_n)}{2} u_j^{(i)} + \frac{P_5}{4Pr} h_j^{-1} \{p_j^n - p_{j-1}^n + p_j^{n-1} - p_{j-1}^{n-1}\} - \frac{\alpha_n}{2} u_{j-1/2}^{n-1}$$

$$(t_8)_j = -\frac{(P_3 + \alpha_n)}{2} u_{j-1}^{(i)} + \frac{P_5}{4Pr} h_j^{-1} \{p_j^n - p_{j-1}^n + p_j^{n-1} - p_{j-1}^{n-1}\} - \frac{\alpha_n}{2} u_{j-1/2}^{n-1}$$

$$(t_9)_j = 0$$

$$(t_{10})_j = 0$$

$$\begin{aligned} (t_{11})_j = & T_{j-1/2}^{n-1} - \frac{1}{Pr} h_j^{-1} (p_j^{(i)} - p_{j-1}^{(i)}) - \frac{(P_1 + \alpha_n)}{2} \{ (f p)_j^{(i)} + (f p)_{j-1}^{(i)} \} \\ & + \frac{(P_3 + \alpha_n)}{2} \{ (u g)_j^{(i)} + (u g)_{j-1}^{(i)} \} - \frac{P_5}{4Pr} h_j^{-1} (g_j^{(i)} - g_{j-1}^{(i)}) \{ p_j^n - p_{j-1}^n + p_j^{n-1} - p_{j-1}^{n-1} \} \\ & - \frac{P_5}{2Pr} h_j^{-1} (p_j^{(i)} - p_{j-1}^{(i)}) g_{j-1/2}^{n-1} - \frac{P_5}{2Pr} \{ (p^2)_j^{(i)} + (p^2)_{j-1}^{(i)} \} - \frac{P_6}{2} \{ (u^2)_j^{(i)} + (u^2)_{j-1}^{(i)} \} - \\ & \frac{\alpha_n}{2} (u_j^{(i)} + u_{j-1}^{(i)}) g_{j-1/2}^{n-1} + \frac{\alpha_n}{2} (g_j^{(i)} - g_{j-1}^{(i)}) u_{j-1/2}^{n-1} + \frac{\alpha_n}{2} (p_j^{(i)} + p_{j-1}^{(i)}) f_{j-1/2}^{n-1} - \\ & \frac{\alpha_n}{2} (f_j^{(i)} + f_{j-1}^{(i)}) p_{j-1/2}^{n-1} \end{aligned} \quad (A28)$$

The boundary conditions (A16) becomes

$$\begin{aligned} \delta f_0^n &= 0, & \delta u_0^n &= 0, \\ \delta p_0^n(\xi, 0) &= \delta \left[\frac{\xi^{1/2} (1 + \xi)^{-1/2} g_0^n - 1}{(1 + \xi)^{-1/2} + \gamma \xi^{1/2} (1 + \xi)^{-2/2} g_0^n} \right], & & (A29) \\ \delta u_1^n &= 0, & \delta g_1^n &= 0 \end{aligned}$$

which just express the requirement for the boundary conditions to remain during the iteration process. Now the system of linear equations (A22), (A23), (A24), (A25) and (A27) together with the boundary conditions (A29) can be written in matrix or vector form, where the coefficient matrix has a block tri-diagonal structure. The whole procedure, namely reduction to first order followed by central difference approximations, Newton's Quasi-linearization method and the block Thomas algorithm, is well known as Keller-box method.

